Functionalized Polyaniline as a Novel Curing Agent For Epoxy Resins

By

Jonathan Cook

A thesis submitted to the Graduate Faculty of
Auburn University
in partial fulfillment of the
requirements for the Degree of
Master of Science

Auburn, Alabama
May 10 , 2015

Keywords: polyaniline, functionalization, composites, epoxy, resin, curing

Approved by

Xinyu Zhang, Chair, Professor of Polymer and Fiber Engineering
Gisela Buschle-Diller, Professor of Polymer and Fiber Engineering
Maria Auad, Professor of Polymer and Fiber Engineering

Abstract

The aim of this project was to functionalize the backbone of polyaniline with amine based nucleophiles to act as a curing agent for epoxy resins. Much work has been done on the use of polyaniline and other intrinsic conducting polymers as functional fillers in composite systems for applications such as corrosion prevention and electromagnetic shielding. However these composites still require the use of volatile amine based curing agents that pose a serious health risk to those producing the materials. Additionally there has been limited investigation into the introduction of reactive functional groups to polyaniline post-polymerization and no examples of polyamine moieties being introduced. The purpose of linking the curing agent and filler together into one material is to eliminate the need for volatile amines when producing composite materials as well as improving the mechanical and thermal properties of the composite system. Polymer functionalization was achieved through a series of solid state oxidations and reductive nucleophilic additions to preserve the morphological features of the polymer and to maximize the number of active amines available for curing. Characterization of the compounds was carried out using ATR-FTIR, UV-Visible spectrometry, and SEM while the thermal properties were evaluated using DSC and TGA. Oxidation of the backbone to the pernigraniline state was confirmed by the increase in intensity of the quinoid imine band at 1580 cm^{-1} and successful attachment of TETA by the reduction of the quinoid imine band and the appearance of sp^3 C-H stretches from 2990 to 2800 cm^{-1} as well as N-H stretching bands from 3500-3300 cm^{-1}.

Acknowledgments

The author would like to thank first and foremost his advisor, Dr. Xinyu Zhang, for the opportunity conduct this work and his enthusiasm, support, and encouragement every step of the way. Secondly, thanks to the committee members Dr. Gisela Buschle-Diller and Dr. Maria Auad for their contributions to this work and their support. The author would like to recognize the Department of Polymer and Fiber Engineering for the support and facilities to conduct this research. Thanks to Steve Moore for assistance with SEM imaging. Special thanks to fellow graduate researchers Bernal Sibaja-Hernandez, Edward Snead and Ricardo Ballestero-Mendez for their advice and moral support. Lastly, the author would like to thank his family for encouraging and supporting his endeavors through all the highs and lows.

Table of Contents

List of Figures

1. INTRODUCTION

Epoxy resins are one of the most significant chemical products in the world today. Resins find use in coatings, industrial and consumer electronics and electrical applications, as well as composites for aerospace, automotive and specialty applications. Global production of epoxy resins is forecasted to reach 30.3 million tons by 2017 and generated $6 billion in 2013 alone, while demand for high quality resins in the US is predicted to grow 10% annually through 2018[1]. With such a wide market and continually growing industry, developments in resins and resin-based composites have the potential for global impact on technology.

One of the main focuses of current research is the formulation of resins with functional fillers such as graphene and carbon nanotubes[2-7], ferromagnetic nanoparticles[8-10], nanoclay[11-14], intrinsically conducting polymers (ICP) [15-20], and combinations of these for a variety of applications. ICPs are multifunctional materials with two major functionalities in composites: corrosion resistance[21-25] and electromagnetic shielding[26-31]. But as with any filler, the introduction of filler materials into the resin-hardener matrix creates defects that ultimately limit the final mechanical properties of the composite.

The aim of this project is to synthesize a polyaniline based ICP filler that will act as a combination functional filler and curing agent. The key focus of the synthetic efforts is to introduce aliphatic polyamines such as triethylenetetramine (TETA) and tris-2(aminoethyl)amine (TRIS) post polymerization in order to maintain morphological control over the bulk polymer.

By introducing these polyamines to the polymer backbone, it will create a pseudo-dendrimer, capable of providing improved thermal and mechanical stability to the composite while maintaining a sufficient loading of functional filler material.

2. LITERATURE REVIEW

2.1 Summary

For optimal curing the functionalized polymer must contain a large number of active hydrogens per repeat unit to provide complete curing as well as covalently linking the filler to the matrix. To achieve this the aliphatic polyamines TETA and TRIS were chosen due to their commercial use as curing agents and the presence of primary amines to act as nucleophiles for attachment to polyaniline.

The proposed synthesis of the functionalized polymer consists of cycles of oxidation, to increase the available sites for the introduction of functional groups, and reductive nucleophilic addition, to attach the polyamines to the polymer (**Figure 1**).

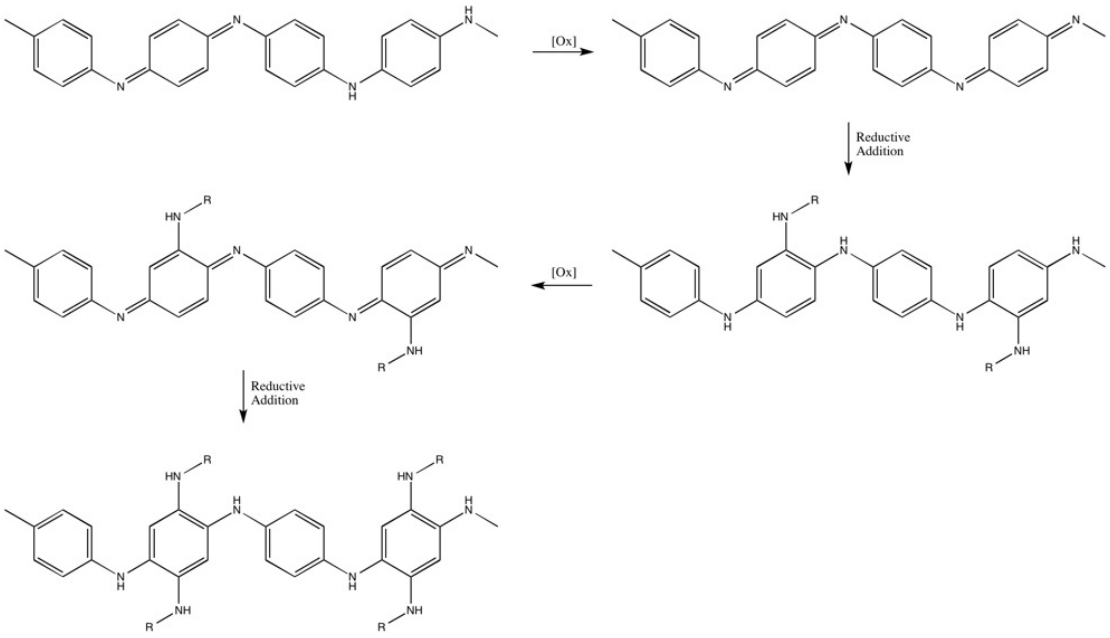

Figure 1. Proposed synthetic scheme

2.2 Conducting polymers

The intrinsically conducting properties of some organic polymers were discovered by MacDiarmid and Shirakawa in the 1970s, the first of which being poly(acetylene) [32], followed by poly(aniline) and poly(pyrrole)[33-34]. It was found that organic polymer backbones comprised of a continuous conjugated network of pi electrons were able to transport charge, exhibiting conductivity in the semiconducting and conducting range. It was also found that exposure to dilute acids improved the conductivity by several orders by providing a dopant counter-ion to stabilize the conducting state[32,,34].

Of these ICPs, poly(aniline) has been one of the most widely studied with thousands of published papers investigating synthetic methodologies, unique morphological architectures, dopant effects, applications for corrosion protection, electromagnetic shielding, chemical sensing, and much more.

2.2.1 Synthetic Methodologies

The two main approaches to poly(aniline) synthesis are chemical oxidative polymerization and electrochemical polymerization[35-39]. While electrochemical polymerization allows for greater control during synthesis through tuning of the voltage potential and the production of uniform thin films, chemical oxidative polymerization easily provides bulk quantities of the polymer and greater opportunity for morphological control. The most common oxidants for the polymerization of polyaniline are ammonium peroxydisulfate (APS) and ferric chloride ($FeCl_3$) and are typically carried out in an acidic aqueous environment[35,40,41]. The reaction proceeds through the oxidation of the monomer to a reactive quinoid structure followed by coupling to an additional unit of monomer to

form the dimer. The dimer is then oxidized by another unit of oxidant and can couple to another monomer or dimer (Figure 2). The cycle repeats to produce dark green precipitate in the reaction vessel that can be isolated by filtration. When carried out in an acidic medium the obtained product is the conductive poly(aniline) emeraldine salt form, and upon treatment with aqueous base the blue poly(aniline) emeraldine base is obtained (Figure 3).

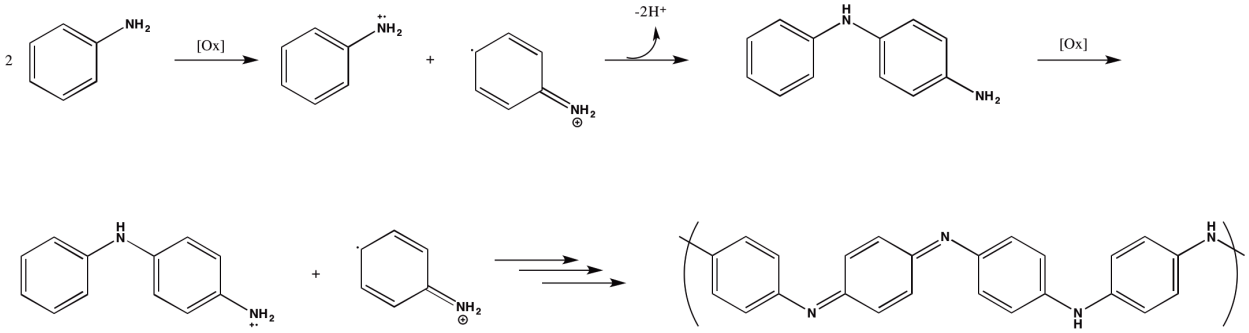

Figure 2. Oxidative polymerization of aniline monomer

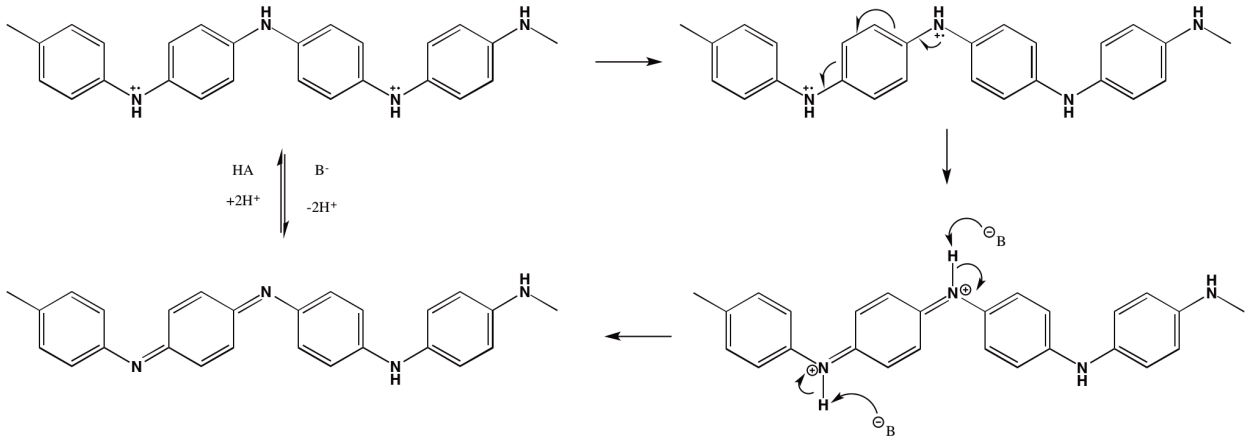

Figure 3. Poly(aniline) doping pathway

In addition to the reversible doping/dedoping, poly(aniline) can also be converted between its three distinct oxidation states (Figure 4) by treatment with oxidants such as APS, H_2O_2, or *m*-CPBA

or reducing agents like hydrazine. The partially oxidized emeraldine salt form exhibits the greatest conductivity due to better charge distribution along the backbone.

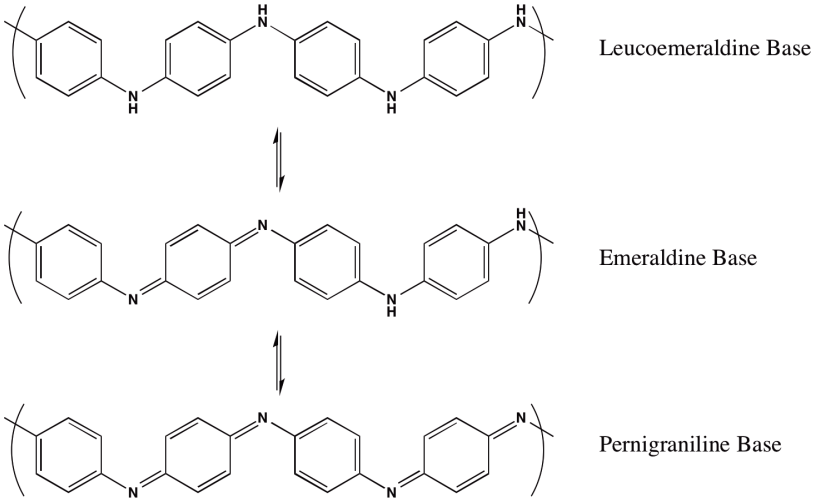

Figure 4. Poly(aniline) oxidation states

2.2.2 Morphological Control

A great deal of work has been done on controlling the morphology of the synthesized poly(aniline) using techniques including interfacial polymerization[42-44], seeding[45,46], surfactant based templating[47,48], and nanoscale self assembly[49-51]. Through these methods a variety of unique nanoscale structures can be produced such as fibers[42,45-47], plates[52,53], spheres [54-55], and urchins [56,57]. These morphologies exhibit interesting chemical and physical properties such as improved conductivity, super-hydrophobicity, and greater chemical sensitivity that can be utilized in a variety of applications such as coatings, sensors and composites.

2.2.3 Applications

The pH responsive nature of poly(aniline) in conjunction with the improved conductivity and increased surface area imparted by its nanofibrous morphology have made poly(aniline) an attractive

new material for an array of sensing applications. To date, poly(aniline) has been used as an effective sensing material for humidity[58], ammonia gas[59], hydrogen sulfide[60], carbon dioxide [61] , and glucose[62].

Poly(aniline) has also been deployed as an anticorrosive agent as both a thin film[63,64] and as an additive in resin based coatings[65,66]. The conductive nature of the polymer channels electrons away from the reactive metal surface preventing oxidation and degradation. These coatings have been used in a variety of marine and structural applications.

Another unique feature of poly(aniline) and some other ICPs is their ability to absorb electromagnetic radiation in the microwave region. This property has found use in synthetic applications for the rapid growth of carbon nanotubes on the surface of engineering materials[67] and reinforcements for composites. When poly(aniline) is used as a filler in epoxy resins, it effectively attenuates electromagnetic waves in the range of 4-18 GHz which corresponds to long range radar and some wireless communication frequencies[68].

2.2.4 Functionalization

Derivatives of poly(aniline) can be prepared using functional monomers containing substituents at the 2, 3, and N position or introducing functional groups post polymerization. Using functional monomers provides access to a wider range of substituents, including halogens[69-71], ethers[72,73], hydroxyl groups[74,75], alkyl[76], and carboxylic acids[77]. The disadvantages are typically lower yields and long reactions times as well as a loss of morphological control.

Introducing functional groups post-polymerization allows for the diverse morphology to be preserved but dramatically limits the potential chemistry that can be performed. The most common

method for the introduction of functional groups is nucleophilic addition to the quinoid ring of the emeraldine or pernigraniline oxidation states[78]. Han and coworkers have demonstrated the reductive addition of simple nucleophiles such as aliphatic amines, thiols and alcohols[79] as well as a unique fluoride catalyzed Michael addition that allows for the introduction of ketones, esters and nitriles[80]. Barbero has shown that addition of sulfate to the backbone of poly(aniline) and poly(N-methylaniline) produces a water soluble derivative that also displays self-doping characteristics[78]. Halogens have also been introduced but require an extremely long reaction time[81]. Addition of phosphines[82] and nitrosyl[83] groups to the nitrogen is also possible but dramatically reduces the conductivity of the polymer.

2.3 Curing Agents

2.3.1 Mechanism of Curing

Curing of epoxy resins requires the interaction of free electrons and active hydrogens with the epoxide rings present in the resin. Nucleophilic attack by the lone pair electrons from a nitrogen, oxygen or sulfur atom opens the reactive epoxide ring, covalently binding the hardener to the resin. A proton shift from the nucleophile to the resin completes the reaction, and in the case of primary amine groups, can undergo a second addition to form further crosslinks. **Figure 5** illustrates the reaction pathway.

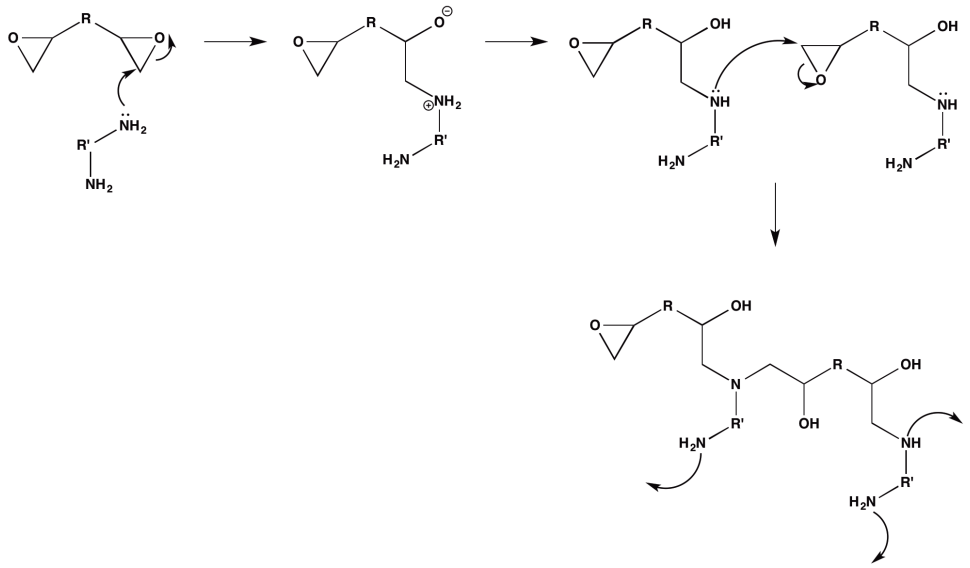

Figure 5. Amine-epoxy curing mechanism

2.3.2 Reactivity and properties of various curing agents

Structures of various curing agents can be seen in Figure 6.

Aliphatic Amines

Aliphatic amines are the most common curing agents for epoxy resin systems, and can be classified as acyclic, alicyclic and aromatic aliphatic. These agents provide room temperature cures and short to moderate pot lives, 30 min to several hours. Resins cured with aliphatic amines have low working temperatures, around 120 ºC, and low resistance to organic solvents.

Aromatic Amines

Aromatic amines react more slowly that their aliphatic counterparts due to reduced basicity and steric interactions with the aromatic ring. Thermal curing is required and usually carried out in two phases, a low temperature initial cure followed by a high temperature. The cured resin has a greater heat stability than its aliphatic counterpart, typically around 150 ºC, and improved solvent and chemical resistance.

Tertiary Amines

Since tertiary amines lack active hydrogens they cannot be used as curing agents on their own, but rather are used as accelerants in conjunction with other curing agents. The presence of the tertiary amine facilitates proton transfers between the joined nucleophile and the opened ring, increasing the kinetics of the rate-limiting step.

Polyamides

Polyamides for curing are comprised of repeating units of secondary amides, usually separated by hydrocarbon chains. Since the nitrogen has only one active hydrogen, the curing times are long but yield a rigid and durable cured resin with excellent mechanical properties.

Thiols

Thiol based curing agents are significantly more reactive than amines, curing at temperatures from 0 ºC to -20 ºC and at times less than 10 minutes, but typically require the use of an accelerator.

Anhydrides

Aromatic, aliphatic and alicyclic anhydrides have all found use as suitable curing agents for large moldings and insulating applications. Alicyclic anhydrides are most commonly used, but all offer good all-around thermal, electrical and mechanical properties. Due to their long pot life, a variety of accelerating agents such as tertiary amines, Lewis acids and organometallics have been employed.

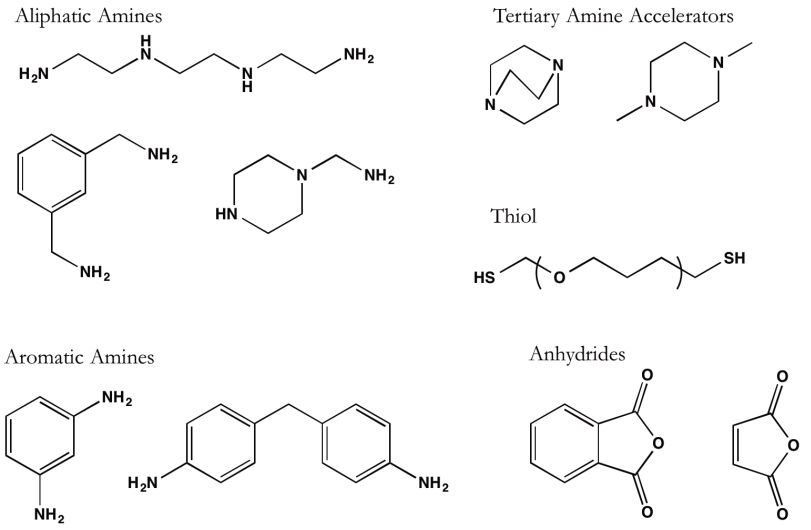

Figure 6. Various structures of curing agents for epoxy resins

2.3.3 Dendritic Curing Agents

Typical curing agents for epoxy resins are low molecular weight aliphatic polyamines such as diethyltriamine, triethylenetetramine, and dipropenediamine. These small molecules offer fast cure times at ambient conditions. Unfortunately these amines are quite volatile and detrimental to human health. One solution to this issue has been the development of low generation dendrimers comprised of aliphatic amines (Figure 7). The heavier dendritic curing agents increase the number of active hydrogens present and the increased molecular weight reduces volatility, thus improving the handling and safety of the curing agent. Additionally, the branched structure allows for a greater number of crosslinks between hardener and resin, which improves the thermal and mechanical stability of the material.

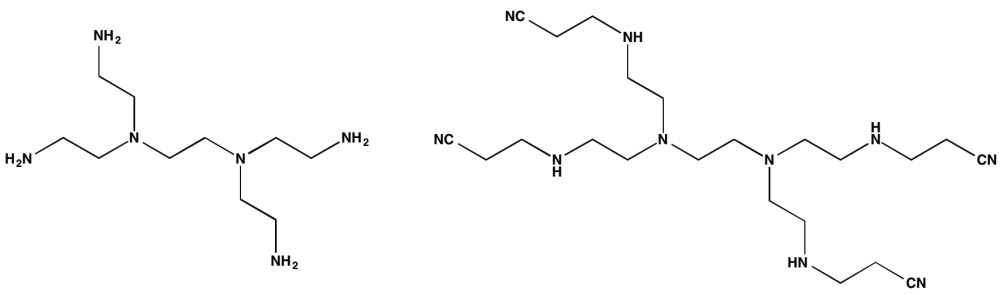

Figure 7. Low generation dendrites for epoxy resin curing

3. EXPERIMENTAL DESIGN

3.1 Materials

Chemicals

Aniline monomer (Alfa Aesar), ammonium peroxydisulfate (Alfa Aesar), triethyltetramine (Acros Organics), and tris-2(aminoethyl)amine (Alfa Aesar) and all solvents were of reagent grade and used as received. EPON 828 resin was produced by Momentive and placed in a water bath at 40 ºC for 2 hrs to remove any crystallization present in the resin.

Characterization

Fourier Transform Infrared Spectroscopy (FTIR) was carried out on a ThermoFisher Nicolet 6700 FT-IR with a Smart Orbit ATR platform. Spectra were compiled from 32 scans at a resolution of 8 cm^{-1}.

UV-Visible Spectroscopy was performed on a Shimadzu UV-2450 and absorbance collected from 200 nm to 900 nm. Solutions were prepared in 1 cm quartz cuvettes using NMP as solvent and blank.

Dynamic Scanning Calorimetry (DSC) was conducted on a TA DSC Q2000 using standard aluminum pans. Non-isothermal curing experiments were performed at various heating rates under nitrogen from 40 ºC to 250 ºC.

Thermal stability measurements were carried out using thermal gravimetric analysis (TGA) on a TA TGA Q500 with platinum pan. The temperature was swept from 25 ºC to 600 ºC at 10 ºC/min, and a nitrogen atmosphere was maintained within the balance and the furnace at a flow rate of 40 mL/min.

Morphology of the polymers and surface characteristics of the composites was imaged using scanning electron microscopy (SEM) with a JSM 7000F backscatter SEM. Samples were mounted on stainless steel studs using carbon tape, and gold coated before imaging.

3.2 Synthesis

3.2.1 Polyaniline Emeraldine Base Nanofibers (PAn EB NF)

In a 1000 mL beaker, 300 mL of aqueous 1M HCl was added followed by aniline monomer (15 mL, 0.1643 mol), which was then placed on high stir. To the solution, 5 mL of V2O5 sol-gel nanofibers was added and allowed to stir for 2 min. APS (17.35 g, 0.0760 mol) in 200 mL of 1M HCl was then added, allowed to stir vigorously for 1 min after which the stir speed was reduced to low. The polymerization was left to proceed for 3 hrs after which it was vacuum filtered to yield a dark green solid, which was washed with excess 1M HCl and acetone. The resulting poly(aniline) emeraldine salt (PAn ES) was dried under vacuum overnight.

To obtain the emeraldine base (PAn EB), PAn ES was ground with mortar and pestle then washed with 1M NH_4OH and water. The resulting dark blue powder was dried under vacuum overnight.

3.2.2 Polyaniline Pernigraniline Base (PAn PB)

0.550 g PAn EB was added to 100 mL of deionized water containing 1 wt.% APS and allowed to stir for 15 min. The solution was filtered, washed with excess deionized water and 1 M NH_4OH. Barbero *et al* noted that when dried, the pernigraniline base was reduced to the 75% nigraniline state. Due to this reduction, the washed PAn PB was carried on to the next reaction without drying. The wet polymer was used to prepare samples for UV-Vis while dried samples were used to collect FTIR data.

3.2.3 Nucleophilic Reductive Addition (PAn-TETA, PAn-TRIS)

In a 100 mL round bottom flask with stir bar, approximately 0.500 g PAn PB was added to 50 mL of 1 M amine in absolute ethanol. The solution was refluxed at 95 ºC for 2 hrs, allowed to cool to room temperature and filtered. The collected solid was washed with deionized water followed by 1 M NH_4OH, then dried under vacuum.

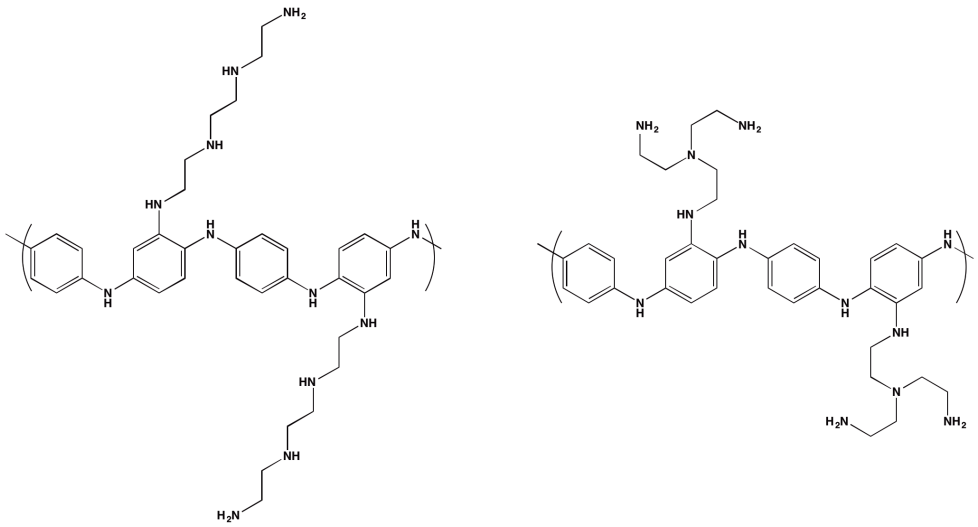

Figure 8. Structures of PAn-TETA (left) and PAn-TRIS (right)

3.2.4 Addition of additional substituents (PAn-TETA2x, PAn-TRIS2x)

Additional oxidations and reductive additions were performed on the substituted polymers using the same methodology outlined above.

3.3 Evaluation of Curing Ability

The parts per hundred ratio (p.h.r.), which determines the weight to weight ratio of epoxide to hardener in proportion to 100 parts epoxide, is calculated using Equation 1.

$$p.h.r.amine = \frac{\frac{MW\ of\ curing\ agent}{\#\ of\ active\ hydrogens} \times 100}{e.e.w\ of\ epoxide} \quad (1)$$

Polyamines TETA and TRIS are structural isomers and both poly(aniline) derivatives have equal numbers of active hydrogens. Working from the idealized structure of the functional polymers, (1) yields a p.h.r. value of 35 parts per hundred. The number of active hydrogens

Samples of EPON 828 and modified poly(aniline) were mixed in the proper ratio and 3-4 mg of the mixture were used for each DSC experiment.

Non-isothermal curing experiments were conducted at 10 ºC, 20 ºC and 30 ºC per minute from 40 ºC to 250 ºC to evaluate the curing ability of the poly(aniline)s and determine optimal curing temperature. Cured resins were subjected to two cycles consisting of heating from 40 ºC to 250 ºC at 10 ºC per minute followed by cooling at 20 ºC per minute back to 40 ºC.

3.3.1 Thermal Stability

The thermal stability of the compounds and resins was evaluated using thermal gravimetric analysis. Experiments were carried out using 3-4 mg of sample and evaluated over the temperature range of 25 ºC to 600 ºC under a nitrogen atmosphere.

4. EXPERIMENTAL RESULTS

4.1 Fourier Transform Infrared Spectroscopy

Following treatment with aqueous oxidant, the infrared spectra of the polymer undergoes several key changes indicating oxidation of the emeraldine state to the nigraniline or pernigraniline form (Figure 9). First, the frequency of the quinoid imine stretch shifted to 1580 cm^{-1} from 1586 cm^{-1} and increased in intensity. Additionally the peak at 1379 cm^{-1}, characteristic to the B-N-Q stretching of PAn EB, disappears. In the fully oxidized pernigraniline state, the intensities of the N=Q=N and N-B-N stretching peaks should be equivalent but upon drying of the pernigraniline polymer, some reductive degradation occurs causing the polymer to approach the 75% nigraniline form. This effect is confirmed by the FTIR results where the ratio of intensity between the peaks is 0.96 for the oxidized polymer and 0.88 for the emeraldine base.

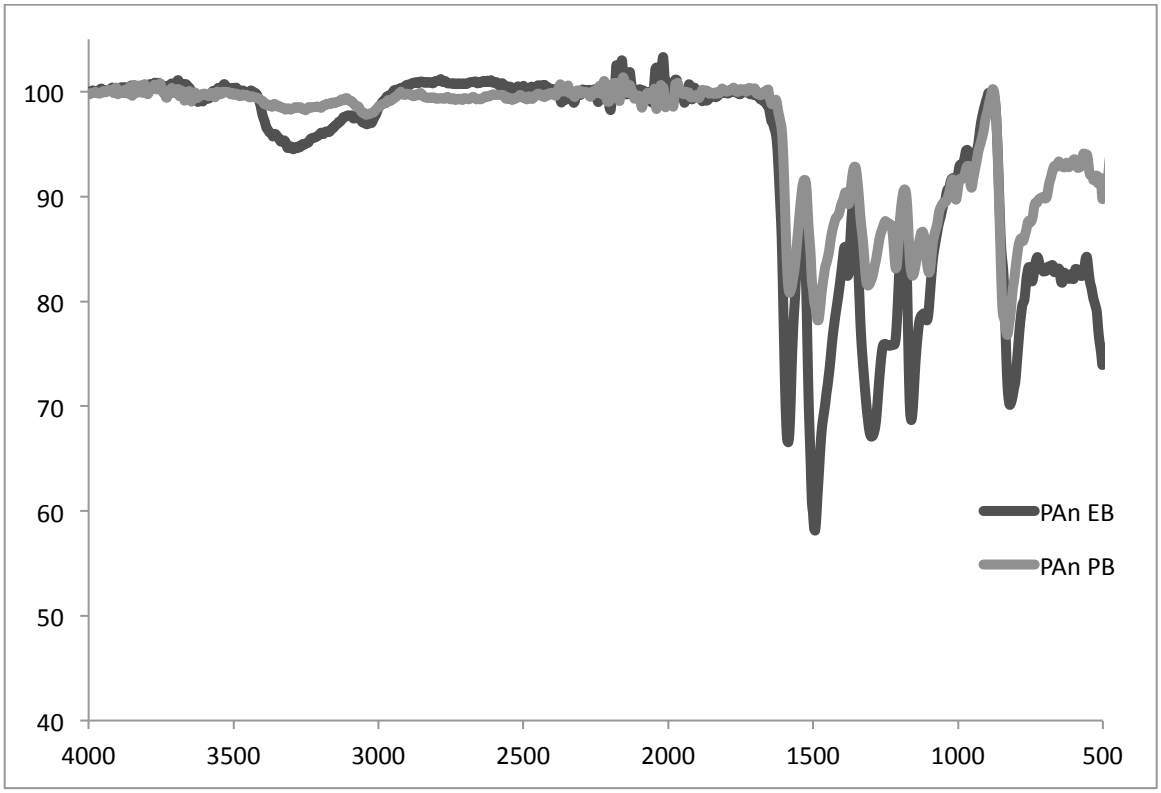

Figure 9. FTIR spectra of poly(aniline) emeraldine and pernigraniline bases

Addition of the nucleophile occurs at the quinoid ring structure of the polymer and results in an overall reduction of the polymer's oxidation state, the intensity of the N=Q=N stretching at 1596 cm^{-1} is greatly diminished in comparison to the pernigraniline base (Figure 10). As expected, the C-H stretching from 2750 to 2950 matches that of the sp^3 carbons of TETA, as well as the change in the 3500-3300 cm^{-1} region brought on by the primary and secondary amine N-H stretches. Since tris-2(aminoethyl)amine is the branched isomer of TETA and as such PAn-TRIS has an almost identical spectrum (Figure 11).

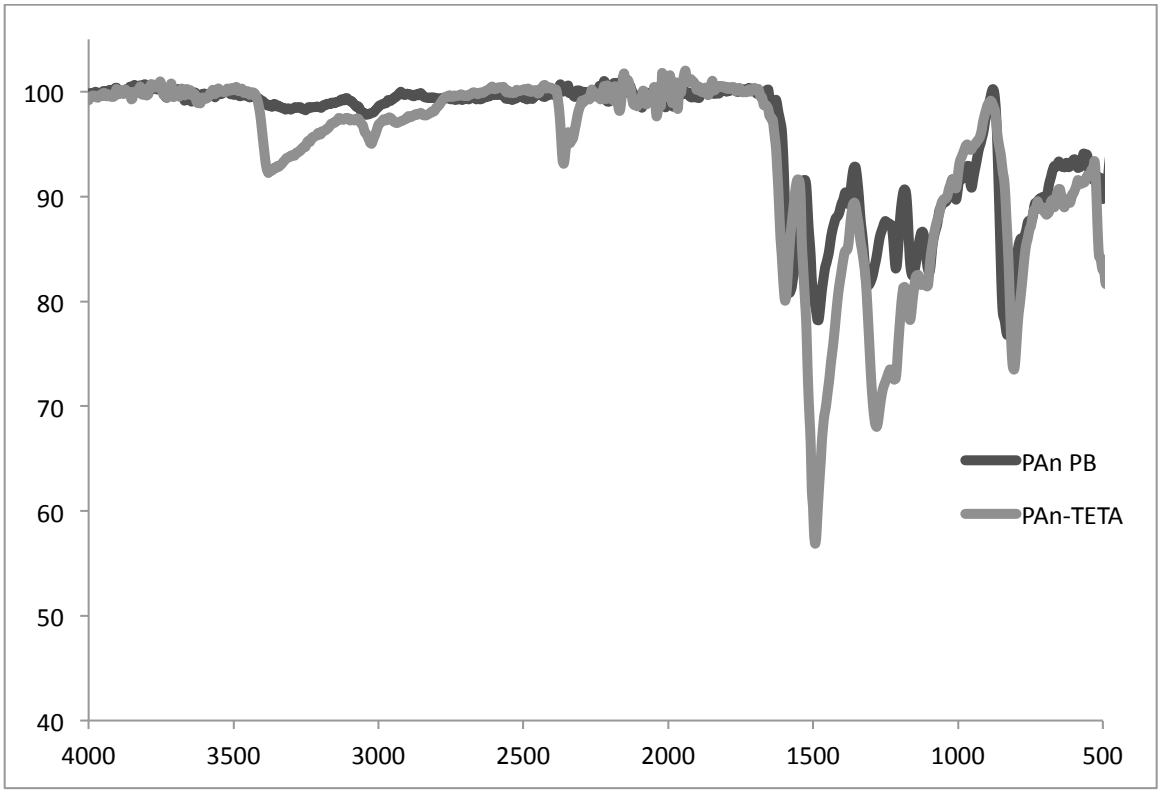

Figure 10. FTIR spectra of poly(aniline) pernigraniline base and TETA adduct

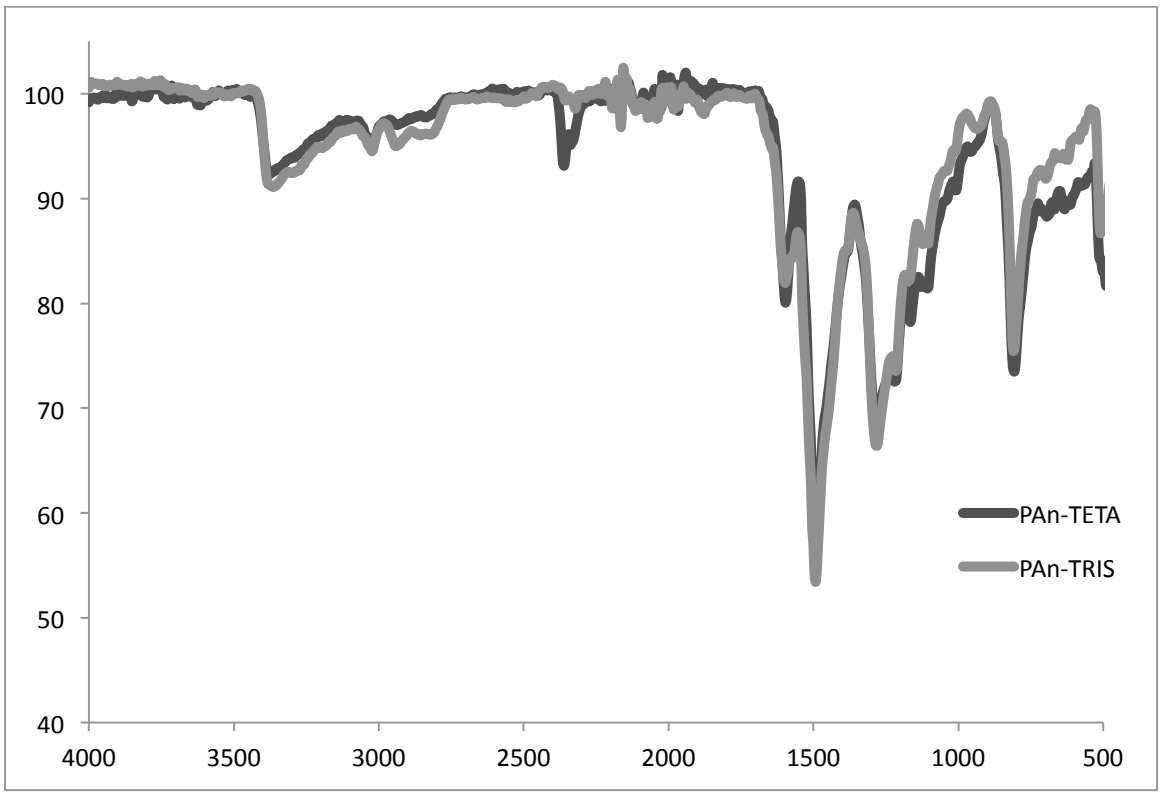

Figure 11. FTIR spectra of polyaniline TETA and TRIS adducts

Attempts to reoxidize the substituted polymer to the emeraldine or pernigraniline states were unsuccessful. Both APS and hydrogen peroxide oxidants were utilized but the resultant material showed loss or degradation of the amine functional group peaks (Figure 12). Oxidation of the polymer backbone did occur, but only to a level near that of the emeraldine state.

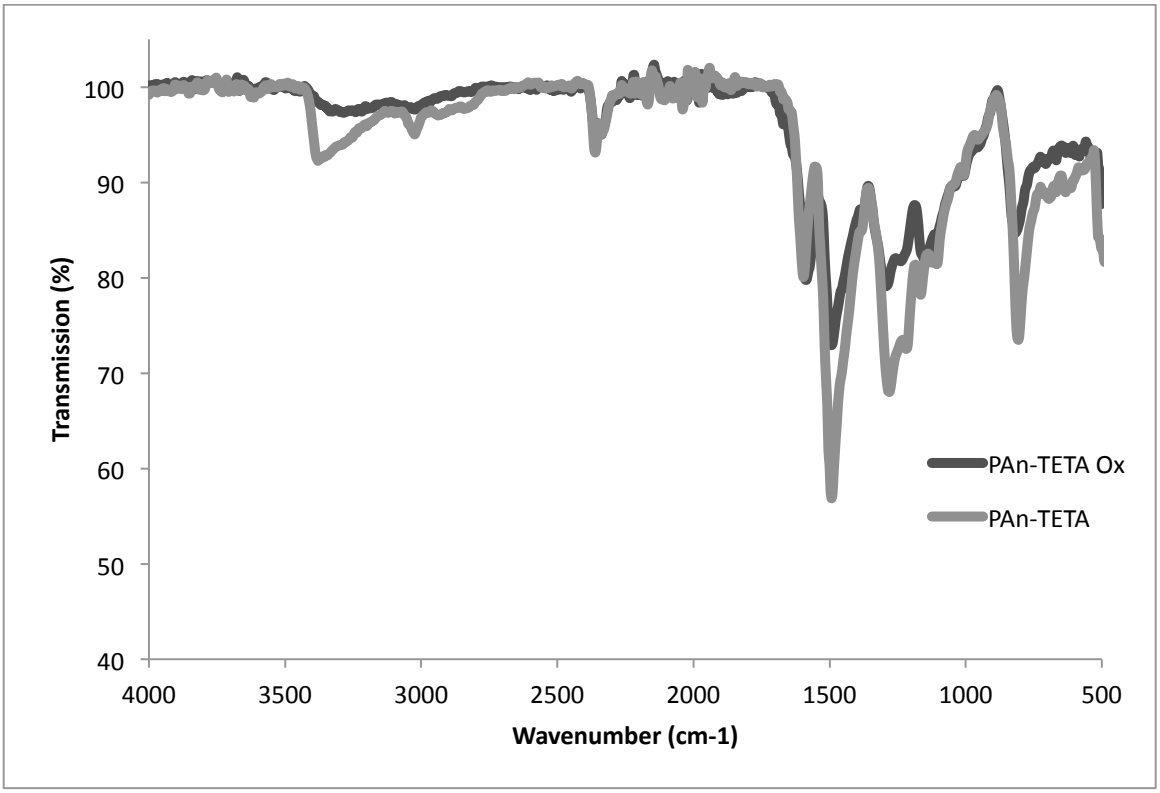

Figure 12. FTIR spectrum of PAn-TETA before and after exposure to aqueous APS

4.2 UV-Visible Spectroscopy

UV-Visible spectroscopy was a key tool in confirming the change in oxidation state of the polymer backbone after each step in the synthesis. Figure 13 displays the shift in absorbance corresponding to the oxidation of the polymer. Both maintain the absorbance peak at approximately 322 nm corresponding to the π-π* transition but after oxidation, the peak at 630 nm shifts to 546 nm. The work by Mattoso and MacDiarmid demonstrated that the shift in intensity and absorbance of the 630 nm peak upon oxidation is strongly correlated to the degree of oxidation of the polymer and arises from a change in the type of electronic transition **REF**. The significant blue shift in the 630 nm peak and no change in the relative intensity of the π-π* transition peak further demonstrate that the emeraldine base has been successfully converted to the pernigraniline base.

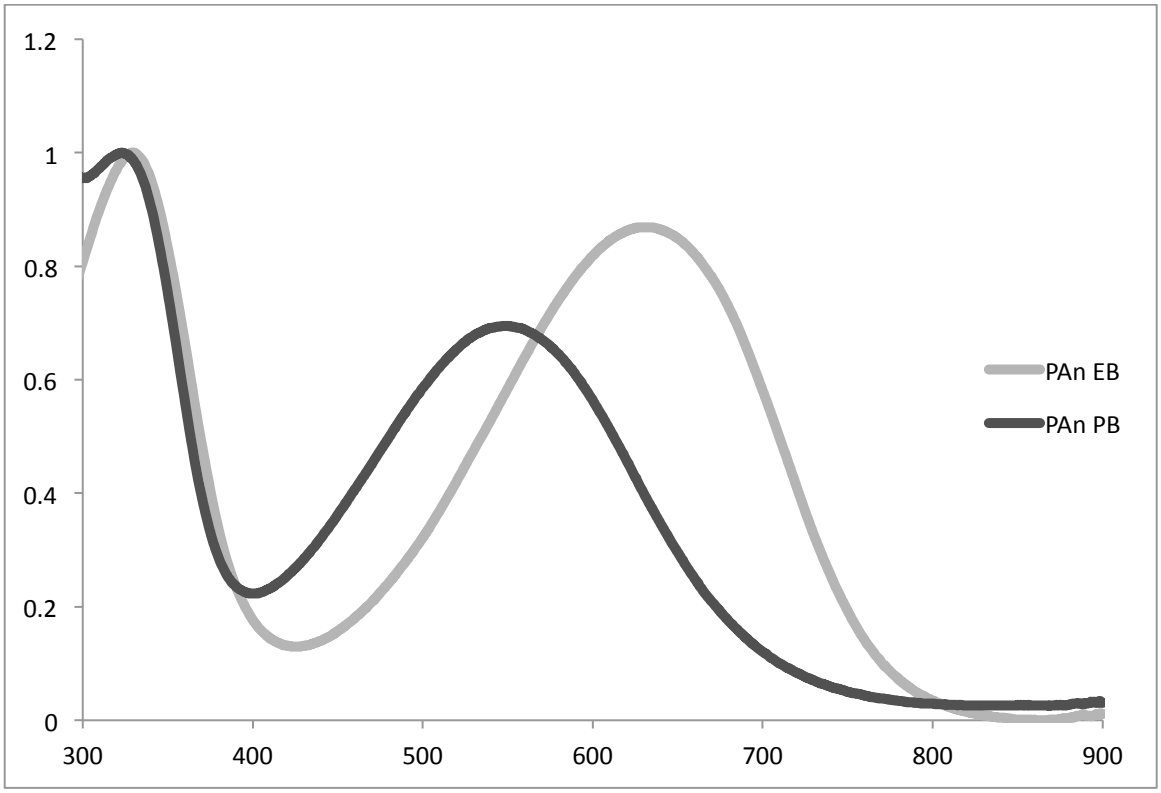

Figure 13. UV-Vis spectrum of poly(aniline) emeraldine and pernigraniline bases

Following reductive addition by the polyamine both peaks in the spectrum were red-shifted (Figure 14). The band at 547 nm returned to the 630 nm absorption seen in the PAn EB but at a significantly lower intensity. Additionally the π-π^* transition band maintained its intensity but shifted in wavelength to 340 nm, common to the transition to the leucoemeraldine state. The red shifting of the 547 nm peak plus the large reduction in relative intensity is indicative of successful reduction of the backbone, brought on by addition of the nucleophile. The TETA and TRIS adducts exhibit near identical spectra indicating equal ability of both nucleophiles to undergo addition, despite structural differences.

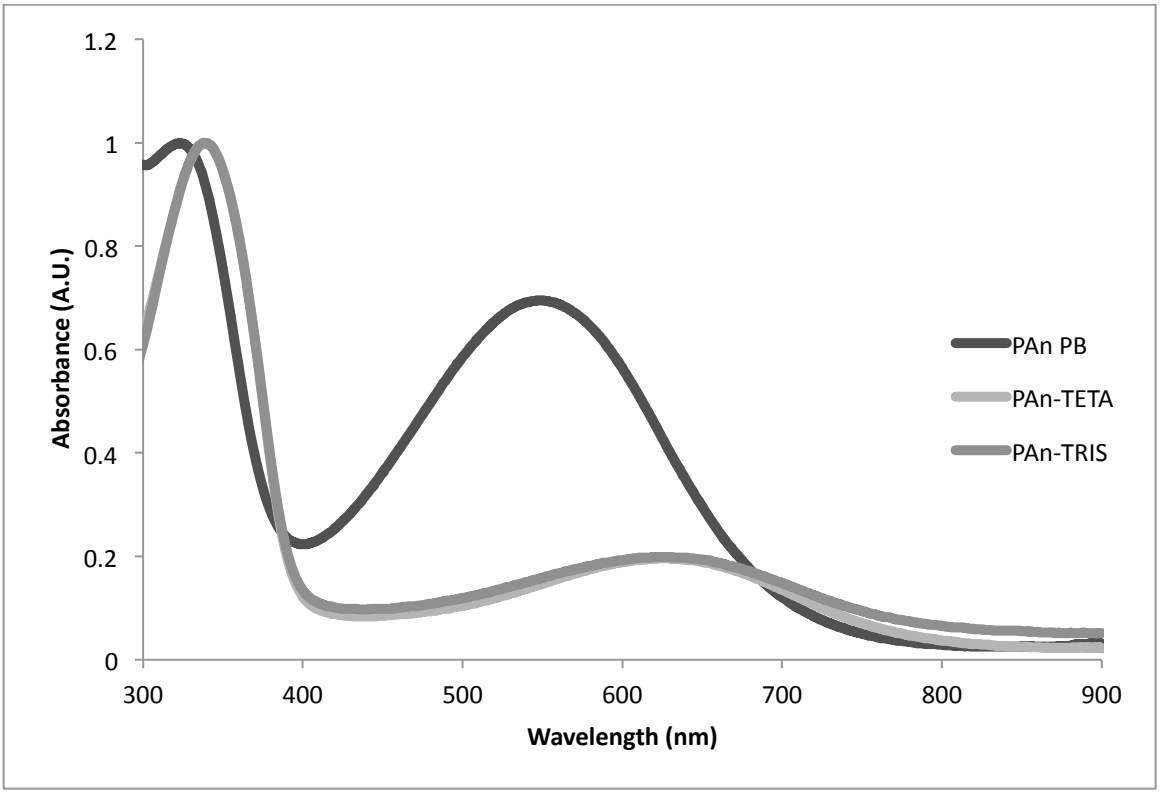

Figure 14. UV-Vis spectrum of poly(aniline) pernigraniline base and polyamine adduct

4.3 Dynamic Scanning Calorimetry

DSC plots indicated that both the emeraldine base and functionalized materials demonstrated curing capabilities at temperatures around 200 ºC, although PAn-TETA and PAn-TRIS displayed a sharper curing peak than that of PAn-EB (Figure 15). When neat epoxy was run through the same conditions, no exothermic curing peak was observed (Figure 16). The curing ability of PAn-EB can be attributed to the presence of secondary amine moieties in the benzoid repeat units of the polymer. However the limited number of available hydrogens and steric hindrance reduces the effectiveness of the emeraldine base as a curing agent, which can be seen in the smaller curing peak in the DSC plot. PAn-TRIS contains two primary amines and one secondary amine in the appended functional group, whereas PAn-TETA contains one

primary amine and three secondary amines. Primary amines are more reactive than secondary amines in the curing reaction, and the greater number of primary amines in PAn-TRIS may account for the lower curing temperature compared to PAn-TETA.

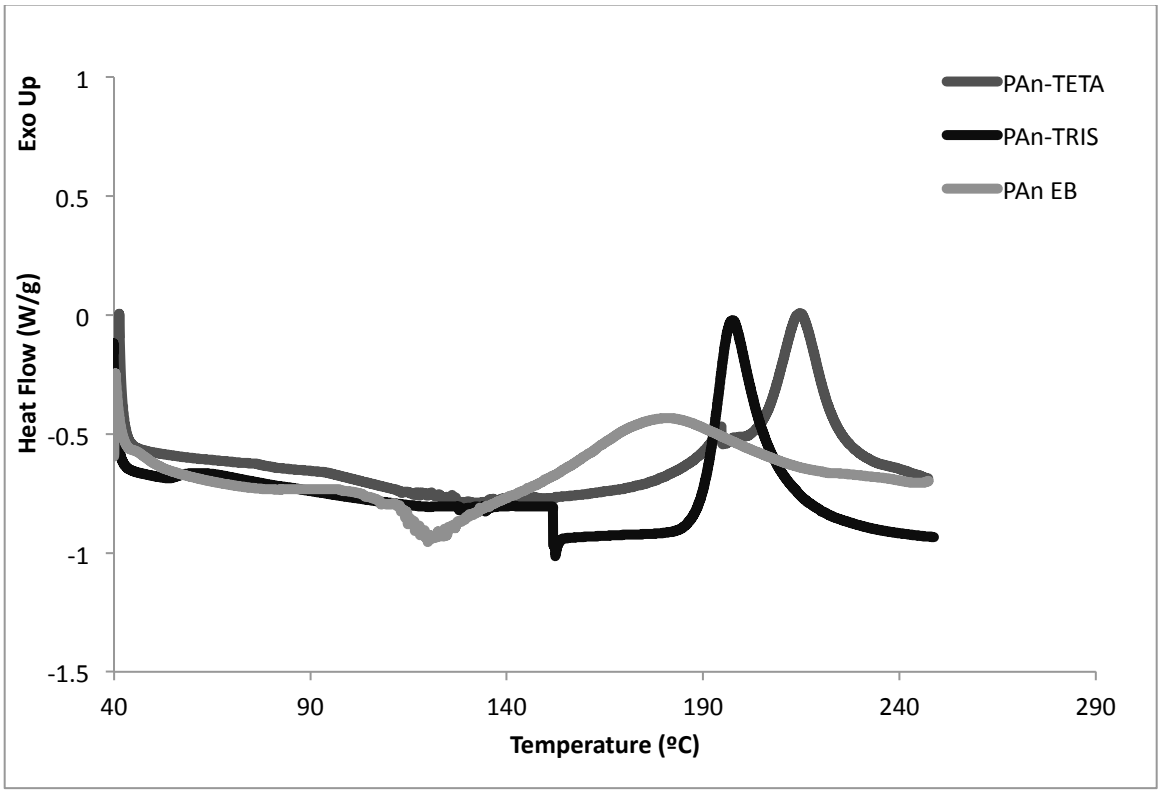

Figure 15. DSC plots for epoxy/poly(aniline) composites at 10 C/min

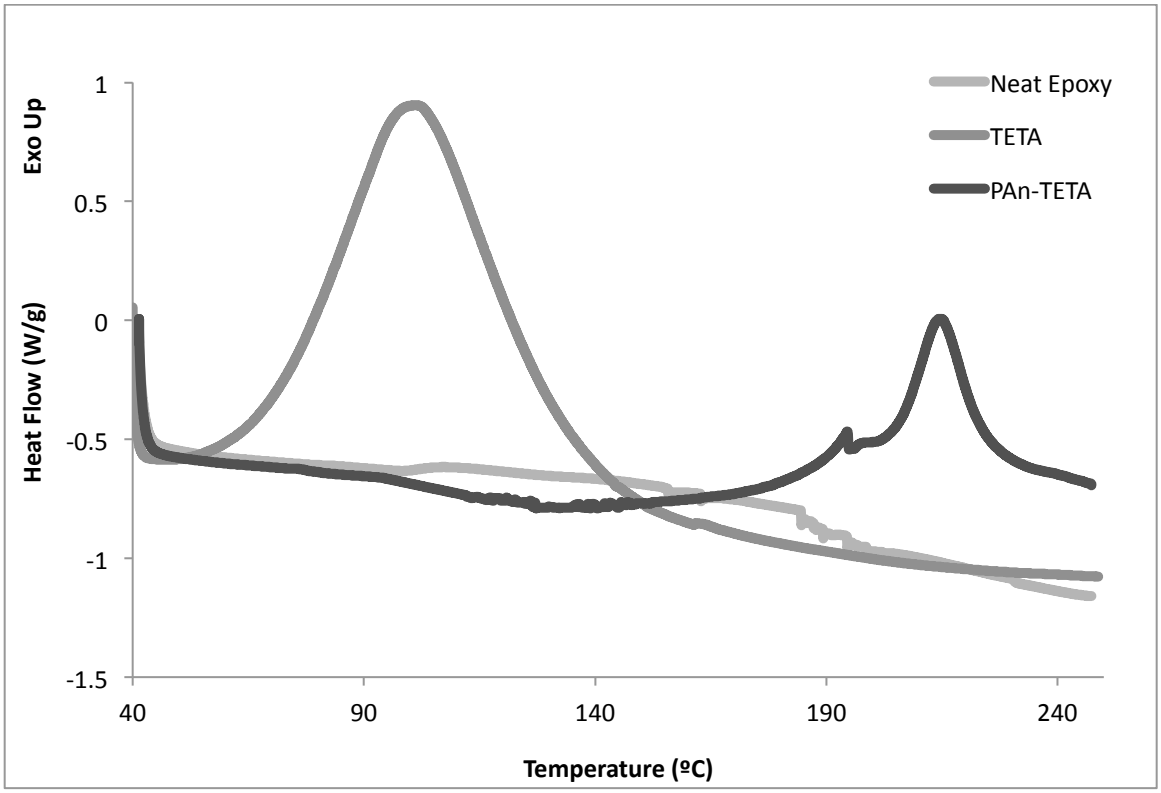

Figure 16. DSC plots of neat epoxy, epoxy/TETA and epoxy PAn-TETA at 10 C/min

4.4 Thermal Gravimetric Analysis

The thermal stability of the epoxy/TETA mixture was used a benchmark to evaluate the performance of the cured poly(aniline) composites. As seen in Figure 17 the epoxy/TETA blend showed no significant weight loss until approximately 280 ºC, and began rapidly decomposing around 310 ºC to 415 ºC. The mass continued to decrease but at a much slower rate until reaching a steady 8.5% mass remaining. The PAn-TETA composite began losing weight at 250 ºC but did not begin to decompose rapidly until approximately 340 ºC. Analysis of the curves found the extrapolated onset of decomposition to occur at 226 ºC for neat epoxy resin, 332 ºC for the epoxy/TETA composite, 351 ºC for the PAn-TETA composite, 347 ºC for the PAn-Tris composite, and 308 ºC for the PAn EB composite. Figure 18 shows the three PAn fillers together

for comparison, PAn-TETA and PAn-TRIS performed very similarly while PAn EB degraded at a lower temperature.

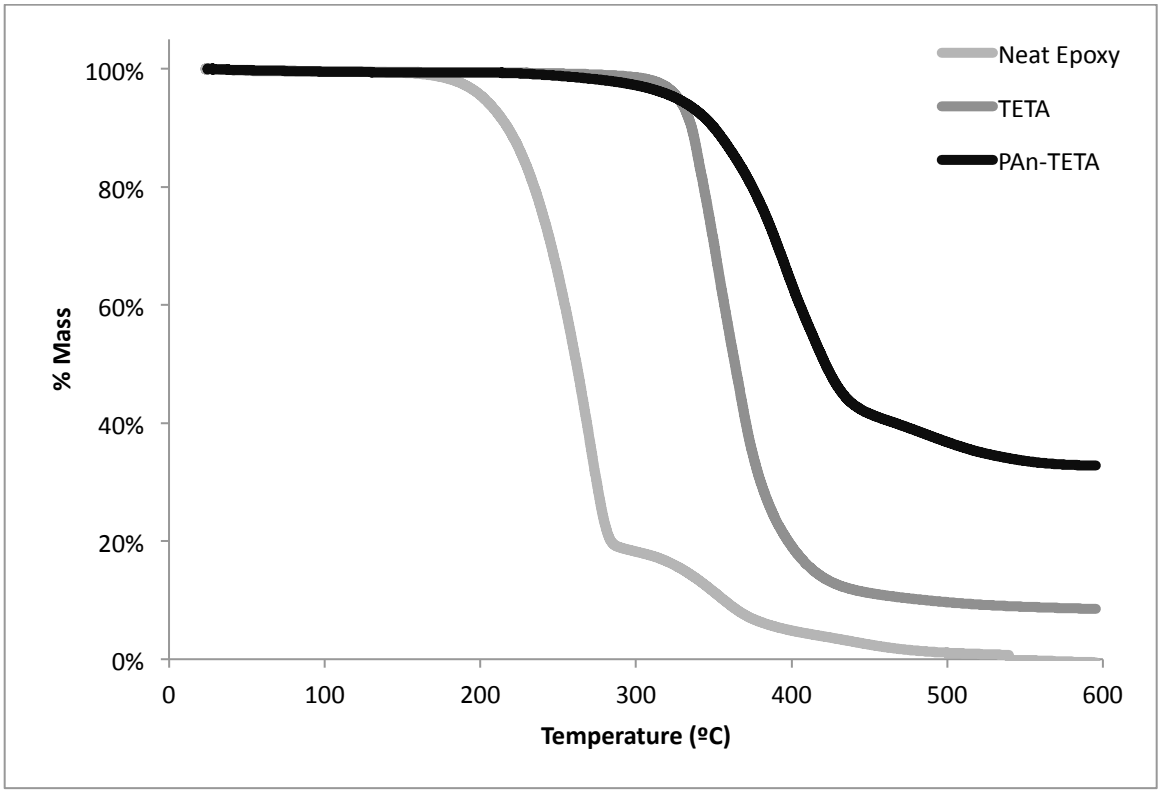

Figure 17. TGA plots of neat epoxy, epoxy/TETA and epoxy/PAn-TETA composites.

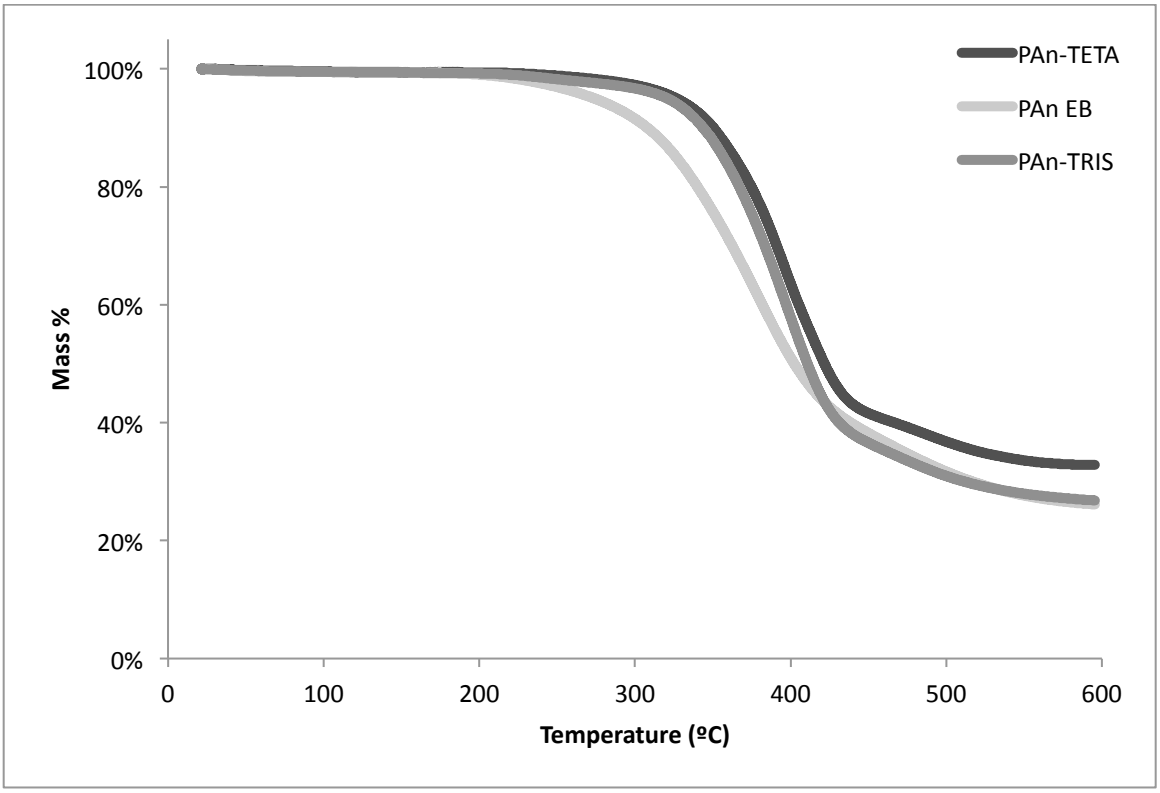

Figure 18. TGA plots of cured epoxy/poly(aniline) composites

In addition to an improvement in the decomposition temperature, the poly(aniline) composite materials also experience less mass loss with PAn-TETA reaching 32% at 600 ºC, PAn-TRIS reaching 27%, and PAn EB with 26% remaining. The rapid decomposition of the TETA composite indicated a homogenous blend of resin and hardener creating one uniform network. The poly(aniline) composites are insoluble in the resin but disperse rather uniformly throughout the mixture. The increase in thermal stability may be a result of covalently binding to the filler and forming a more durable network.

4.5 Scanning Electron Microscopy

SEM was used to confirm the morphology of the starting material and investigate any changes to the physical structure that may have taken place in the course of synthesis. As seen in Figure 19 and

Figure 20, the nanofiber seeded poly(aniline) emeraldine base only formed short, stubby fibers more akin to rods than fine nanofibers. The lack of abundant, high aspect ratio fibers may result from too low a concentration of nanofiber seeds during synthesis, or possibly damage during grinding of the polymer.

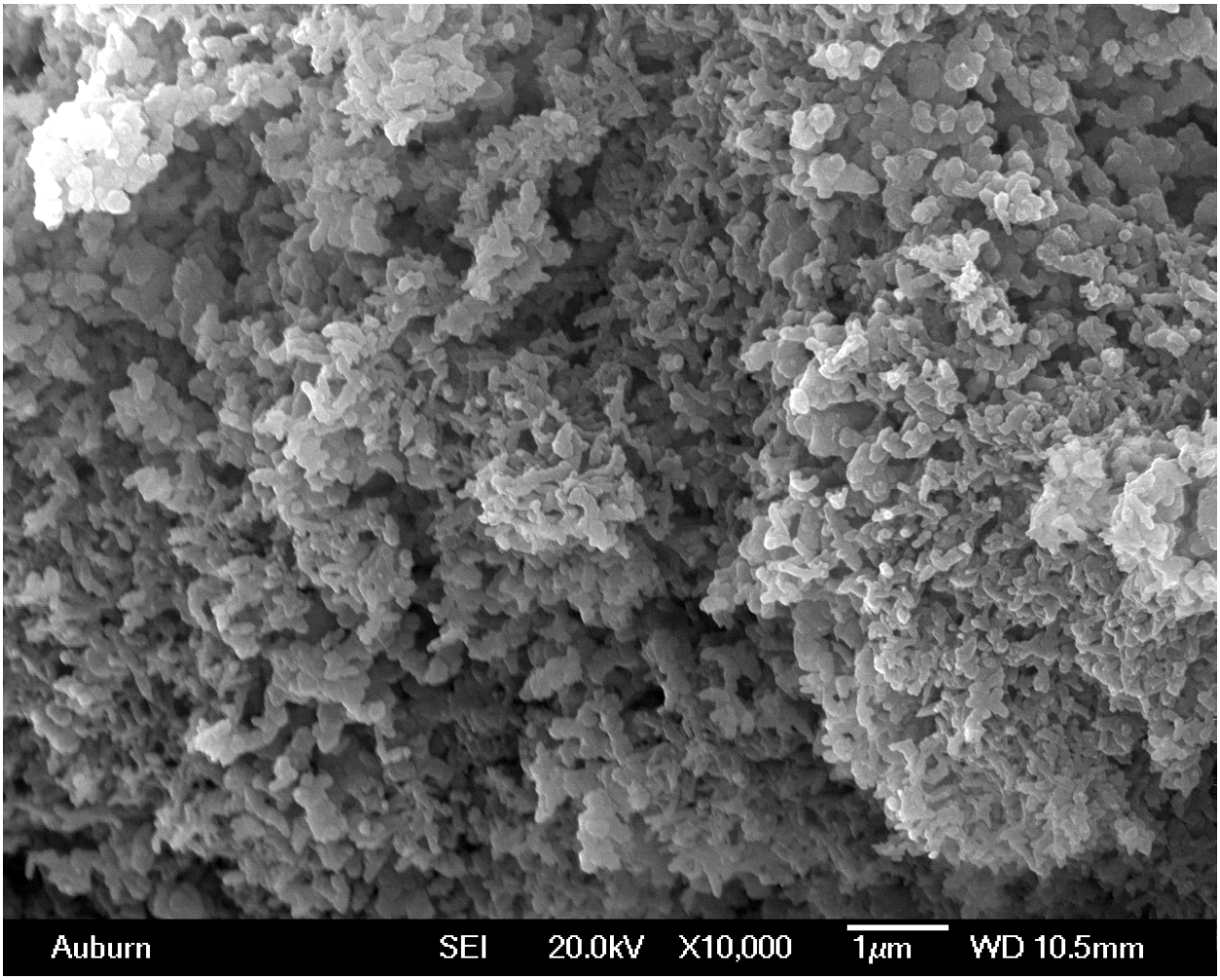

Figure 19. SEM image of PAn EB synthesized via nanofiber seeding

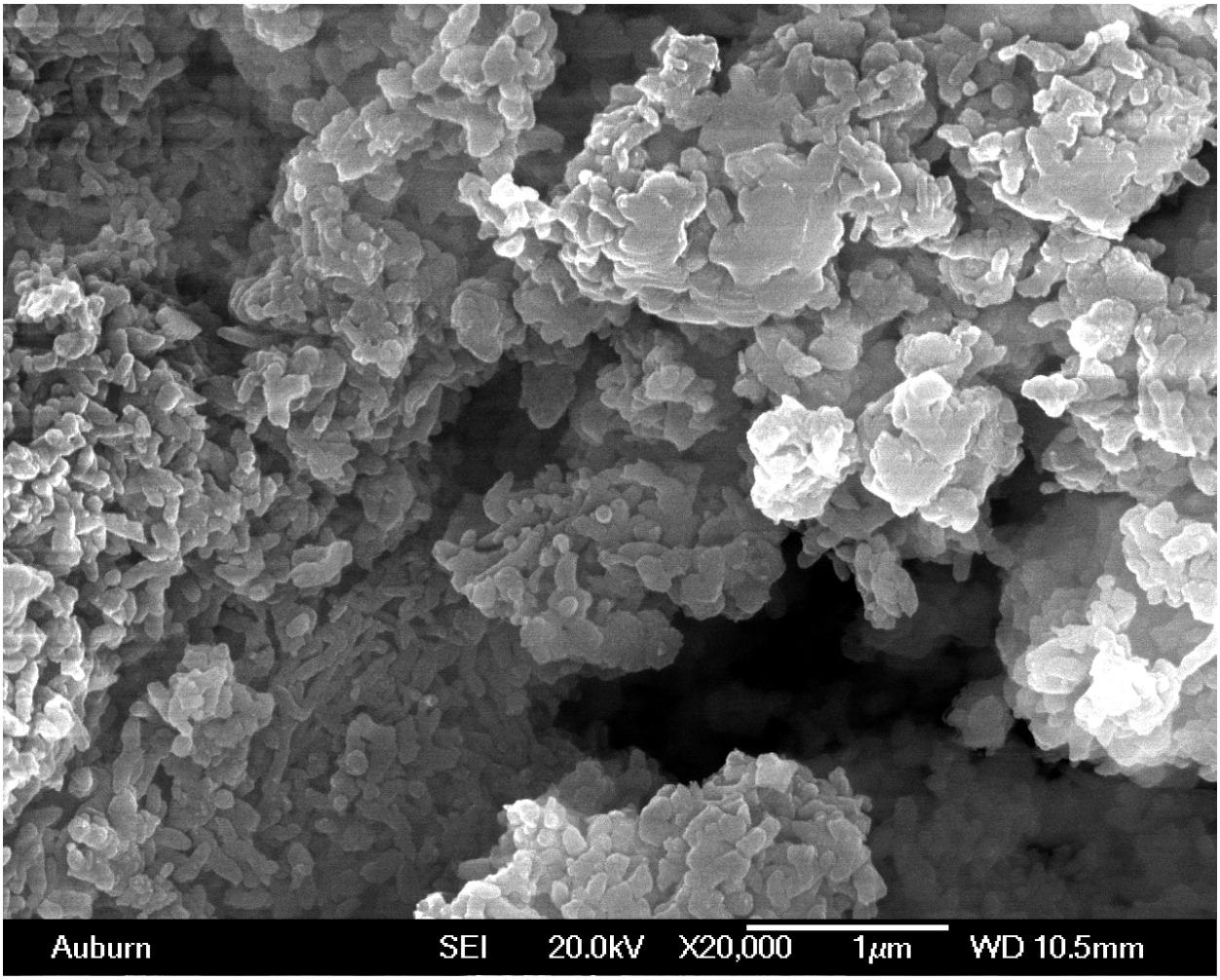

Figure 20. SEM image of PAn EB synthesized via nanofiber seeding

Despite the state of nanofibers in the starting material, following reductive addition of the amine to the polymer, the morphology underwent a change to a flower-like architecture comprised of thin interconnected blades (Figure 21). The flower-like clusters were 1-2 μm in diameter, with the component blades being 25-50 nm in thickness. Figure 22 shows what appear to be nodules of approximately 200 nm diameters with early stages of blade growth evident. The presence of these nodules in proximity to fully developed flower architectures suggests that aggregated knots of short nanofibers may act as seedlings for self-assembly or transition to the flower morphology. Also of

note are observable cracks in the blades of the flower structures (Figure 23), however the cause of these cracks and the morphological shift are not fully understood at this time

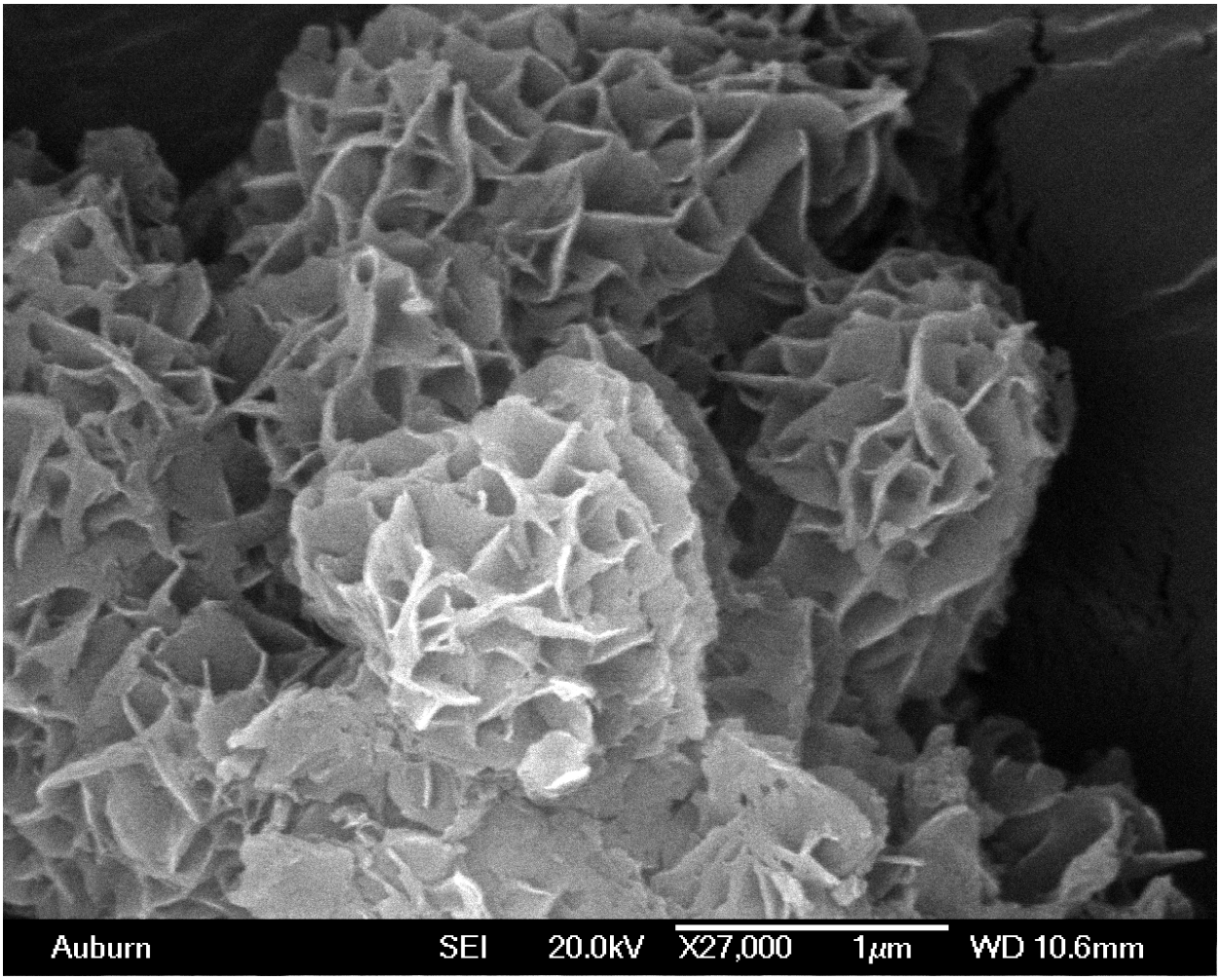

Figure 21. SEM image of PAn-TETA nanoflowers

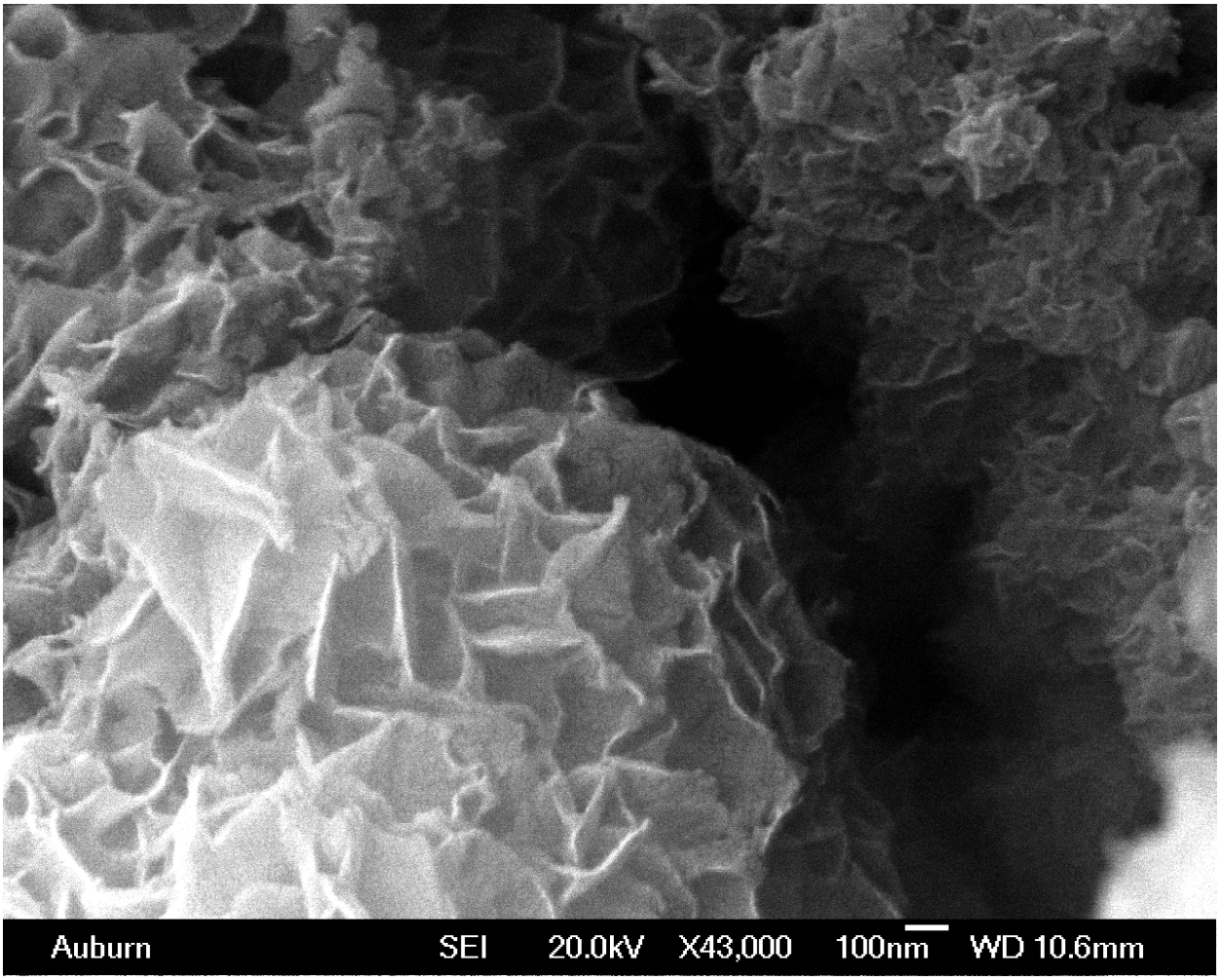

Figure 22. PAn-TETA nanoflowers and seedling nodules

Figure 23. PAn-TETA nanoflowers with visible cracks in blades

The cured composite was also examined to determine the surface characteristics as well observation of the fracture surface to determine the dispersion of poly(aniline) fillers in the composite. Figure 24 and Figure 25 show that the non-mold side of the composite is rough, with visible bumps from the polymer dispersion. Pits and crags on the fracture surface also indicate that the filler is dispersed uniformly throughout the matrix and that bonding between the filler is fairly strong.

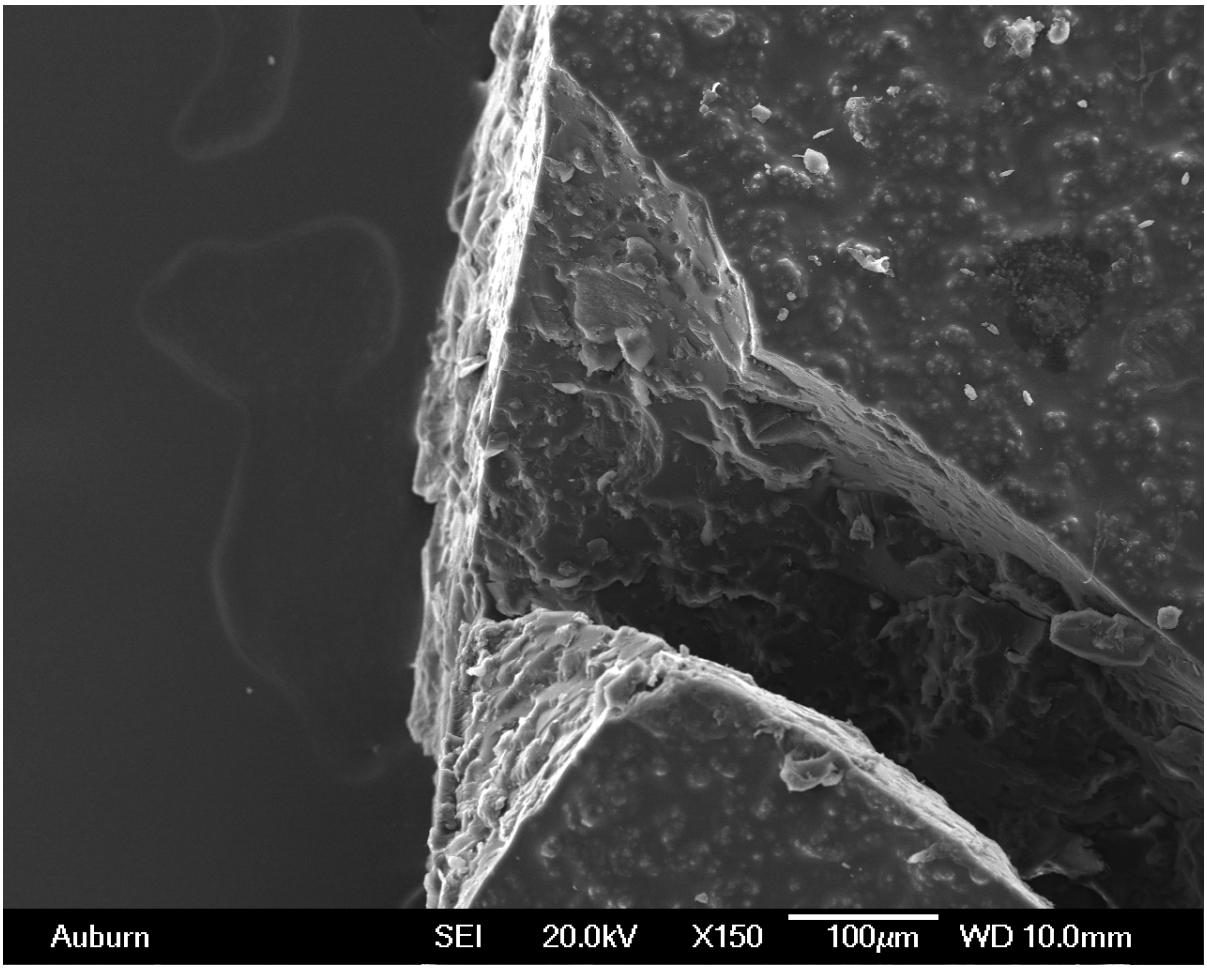

Figure 24. Fracture surface of epoxy/PAn-TETA composite

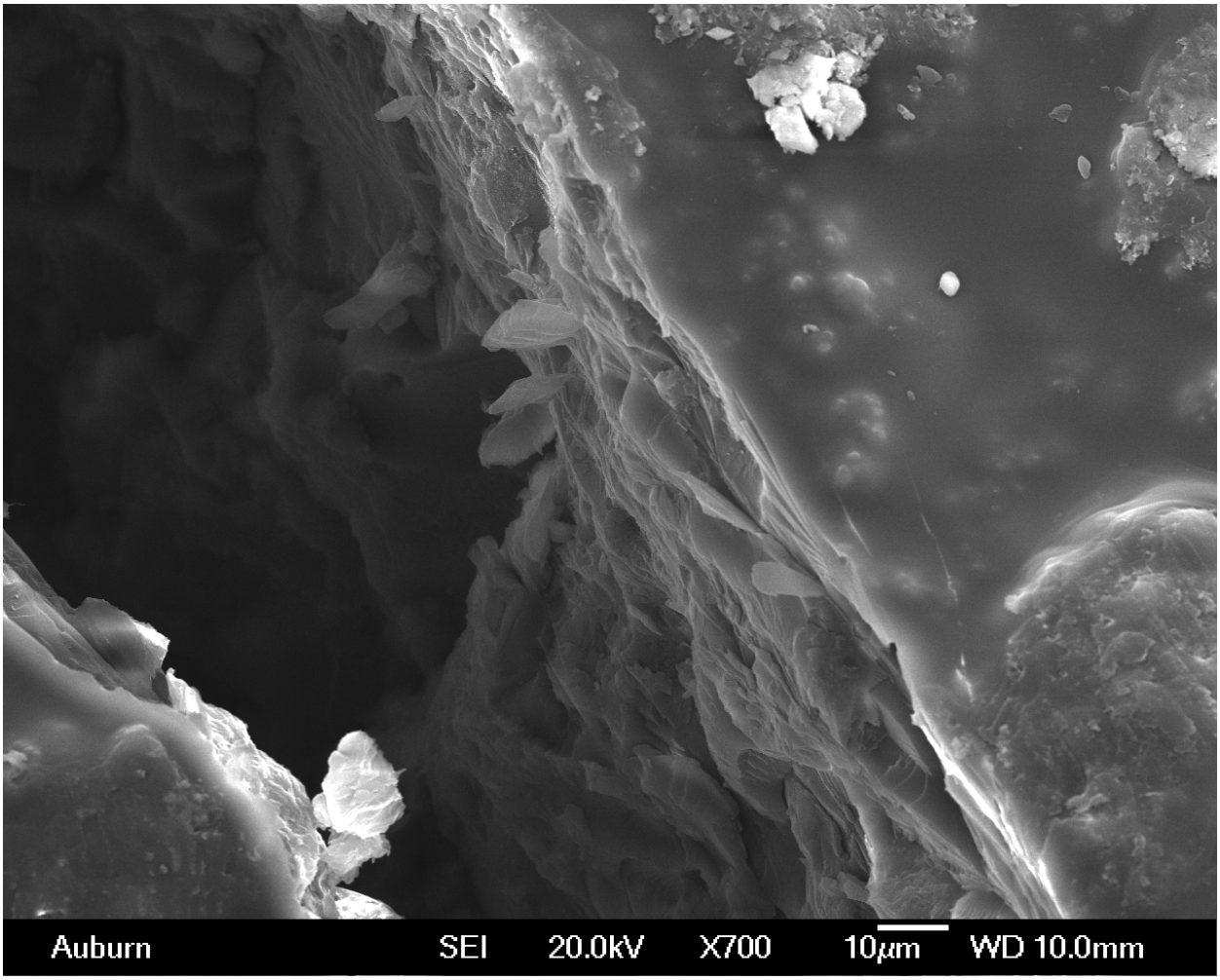

Figure 25. Fracture surface of epoxy/PAn-TETA composite

5. CONCLUSIONS

Poly(aniline) has been successfully modified through covalent attachment of aliphatic polyamines to the backbone via a two step process, oxidation to the fully oxidized pernigraniline state followed by reductive addition by the polyamine nucleophile. UV-visible and FTIR spectroscopy were employed to characterize the polymer, while DSC was used to determine the curing behavior of the functionalized polyaniline-epoxy system.

The theoretical optimum ratio of epoxy to PAn-TETA or PAn-TRIS was found to be 100:35 (wt./wt.), and composite samples were produced. Poly(aniline) emeraldine base also exhibited some curing capabilities due to the presence of secondary amines in the backbone of the polymer but DSC and TGA experiments revealed that it was inferior to both of the functionalized derivatives produced. The peak curing temperature for PAn-TETA and PAn-TRIS was 215 ºC and 198 ºC respectively, much higher than the 100 ºC peak temperature of the epoxy/TETA mixture.

SEM imaging revealed a unique morphological shift from short nanofibers to large three-dimensional flower-like structures after reductive addition by polyamine nucleophiles. Additionally, the poly(aniline) additives were well dispersed throughout the composite and the rough fracture surface indicated good adhesion between matrix and filler.

Both poly(aniline) derivatives produced a solid and stable final composite, and represent the first example of a poly(aniline) derivative produced post-polymerization to be used for this application.

6. RECOMMENDATIONS FOR FUTURE WORK

The first objective for future work will be improvement in the nanofiber morphology of the poly(aniline) emeraldine base starting material and investigation of the observed morphological transition to the 3-D flower like architecture. Additional morphologies of the starting material and various polyamines should be investigated to explore the origin of the morphological transition, as well as on the final properties of the composite.

Exploration of polyamine and morphology combinations may also provide improved curing temperatures which is of great interest. Additionally the mechanical and electrical properties of the functional poly(aniline)s should also be investigated to determine the optimal end use of this new material.

REFERENCES

1. Chemical Economics Handbook: Epoxy Resins, HIS Inc., May, 2014
2. S. Yang, W. Lin, Y. Huang, H. Tien, J. Wang, C. M. Ma, S. Li, Y. Wang, *Synergetic effects of graphene platelets and carbon nanotubes on the mechanical and thermal properties of epoxy composites,* Carbon, 2011, **49**(3), 793-803.
3. J. Liang, Y. Wang, Y. Huang, Y. Ma, Z. Liu, J. Cai, C. Zhang, H. Gao, Y. Chen, *Electromagnetic interference shielding of graphene/epoxy composites*, Carbon, 2009, **47**(3), 922-925.
4. C. Teng, C. M. Ma, C. Lu, S. Yang, S. Lee, M. Hsiao, M. Yen, K. Chiou, T. Lee, *Thermal conductivity and structure of non-covalent functionalized graphene/epoxy composites*, Carbon, 2011, **49**(15), 5107-5111.
5. L.S. Schadler, S.C. Giannaris, P.M. Ajayan., *Load transfer in carbon nanotube epoxy composites*, Applied Physics Letters, 1998, **73**, 3842-3844.
6. D.R. Bortz, E.G. Heras, I. Martin-Gullon, *Impressive Fatigue Life and Fracture Toughness Improvements in Graphene Oxide/Epoxy Composites*, Macromolecules, 2012, **45** (1), 238-245
7. S. Chatterjee, J.W. Wang, W.S. Kuo, N.H. Tai, C. Salzmann, W.L. Li, R. Hollertz, F.A. Nüesch, B.T.T. Chu, *Mechanical reinforcement and thermal conductivity in expanded graphene nanoplatelets reinforced epoxy composites*, Chemical Physics Letters, 2012, **531**, 6-10
8. C. Nan, D.R. Clarke, *Effective properties of ferroelectric and/or ferromagnetic composites: a unified approach and its application*, Journal of the American Ceramic Society, 1997, **80** (6), 1333-1340.
9. L.A. Ramajo, A.A. Cristóbal, P.M. Botta, J.M. Porto López, M.M. Reboredo, M.S. Castro, *Dielectric and magnetic response of Fe3O4/epoxy composites*, Composites Part A: Applied Science and Manufacturing, 2009, **40**(4), 388-393.

10. D. Zhao, X. Li, Z. Shen, *Microwave absorbing property and complex permittivity and permeability of epoxy composites containing Ni-coated and Ag filled carbon nanotubes*, Composites Science and Technology, 2008, **68**(14), 2902-2908

11. J.F. Timmerman, B.S. Hayes, J.C. Seferis, *Nanoclay reinforcement effects on the cryogenic microcracking of carbon fiber/epoxy composites*, 2002, **62**(9), 1249-1258

12. C. Lam, K. Lau, H. Cheung, H. Ling, *Effect of ultrasound sonication in nanoclay clusters of nanoclay/epoxy composites*, Materials Letters, 2005, **59**(11), 1369-1372

13. C. Lam, H. Cheung, K. Lau, L. Zhou, M. Ho, D. Hui, *Cluster size effect in hardness of nanoclay/epoxy composites*, Composites Part B: Engineering, 2005, **36**(3), 263-269

14. S. Ullah Khan, A. Munir, R. Hussain, J. Kim, *Fatigue damage behaviors of carbon fiber-reinforced epoxy composites containing nanoclay*, Composites Science and Technology, 2010, **70**(14), 2077-2085

15. J. Lu, K. Moon, B. Kim, C.P. Wong, *High dielectric constant polyaniline/epoxy composites via in situ polymerization for embedded capacitor applications*, Polymer, 2007, **48**(6), 1510-1516

16. M. Tiitu, A. Talo, O. Forsén, O. Ikkala, *Aminic epoxy resin hardeners as reactive solvents for conjugated polymers: polyaniline base/epoxy composites for anticorrosion coatings*, Polymer, 2005, **46**(18), 6855-6861

17. X. Yang, T. Zhao, Y. Yu, Y. Wei, *Synthesis of conductive polyaniline/epoxy resin composites: doping of the interpenetrating network*, Synthetic Metals, 2004, **142**, 57-61

18. J. Fournier, G. Boiteux, G. Seytre, G. Marichy, *Percolation network of polypyrrole in conducting polymer composites*, Synthetic Metals, 1997, **84**, 839-840

19. C. Cassignol, M. Cavarero, A. Boudet, A. Ricard, *Microstructure–conductivity relationship in conducting polypyrrole/epoxy composites*, Polymer, 1999, **40**(5), 1139-1151

20. O. Zabihi, A. Khodabandeh, S.M. Mostafavi, *Preparation, optimization and thermal characterization of a novel conductive thermoset nanocomposite containing polythiophene nanoparticles using dynamic thermal analysis*, Polymer Degradation and Stability, 2012, **97**(1), 3-13

21. R.C. Patil, S. Radhakrishnan, *Conducting polymer based hybrid nano-composites for enhanced corrosion protective coatings*, Progress in Organic Coatings, 2006, **57**(4), 332-336

22. J.I. Iribarren, E. Armelin, F. Liesa, J. Casanovas, C. Aleman, *On the use of conducting polymers to improve the resistance against corrosion of paints based on polyurethane resins*, Materials and Corrosion, 2006, 57(9), 683-688

23. J.I. Iribarren, F. Cadena Villota, F. Liesa, *Corrosion protection of carbon steel with thermoplastic coatings and alkyd resins containing polyaniline as conductive polymer*, Progress in Organic Coatings, 2005, **52**(2) 151-160

24. E. Armelin, R. Pla, F. Liesa, X. Ramis, José I. Iribarren, Carlos Alemán, *Corrosion protection with polyaniline and polypyrrole as anticorrosive additives for epoxy paint*, Corrosion Science, 2008, **50**(3), 721-728

25. H Nguyen Thi Le, B Garcia, C Deslouis, Q Le Xuan, *Corrosion protection and conducting polymers: polypyrrole films on iron*, Electrochimica Acta, 2001, **46**(26), 4259-4272

26. Y. Wang, X. Jing, *Intrinsically conducting polymers for electromagnetic interference shielding*, Polym. Adv. Technol. 2005, **16**(4), 344-351

27. M Paligová, J Vilčákova, P Sáha, V Křesálek, J Stejskal, O Quadrat, *Electromagnetic shielding of epoxy resin composites containing carbon fibers coated with polyaniline base*, Physica A: Statistical Mechanics and its Applications, 2004, **335**(3), 421-429

28. J. Joo, A.J. Epstein, *Electromagnetic radiation shielding by intrinsically conducting polymers* Applied Physics Letters, 1994, **65**, 2278-2280

29. S.K Dhawan, N Singh, S Venkatachalam, *Shielding behaviour of conducting polymer-coated fabrics in X-band, W-band and radio frequency range*, Synthetic Metals, 2002, **129**(3), 261-267

30. S.K. Dhawan, N Singh, D Rodrigues, *Electromagnetic shielding behaviour of conducting polyaniline composites*, Science and Technology of Advanced Materials, 2003, **4**(2), 105-113

31. N.F. Colaneri, L.W. Schacklette, *EMI shielding measurements of conductive polymer blends*, IEEE Transactions on Instrumentation and Measurement, 1992, **41**(2,) 291-297

32. H. Shirakawa, E. J. Louis, A. G. MacDiarmid, C. K. Chiang, A. J. Heeger, *Synthesis of electrically conducting organic polymers: polyacetylene, (CH)x*, J.C.S. Chem. Commun. 1997, 578-580

33. J. Chiang, A.G. MacDiarmid, '*Polyaniline': Protonic acid doping of the emeraldine form to the metallic regime*, Synthetic Metals, 1986, **13**(1), 193-205

34. A.G. MacDiarmid, *"Synthetic Metals": A Novel Role for Organic Polymers (Nobel Lecture).* Angewandte Chemie International Edition, 2001, **40(14)**, 2581-2590

35. M. Delvaux, J. Duchet, P. Stavaux, R. Legras, S. Demoustier-Champagne, *Chemical and electrochemical synthesis of polyaniline micro- and nano-tubules*, Synthetic Metals, 2000, **113**(3), 275-280

36. L.J. Duic, Z. Mandic, F. Kovacicek, *The effect of supporting electrolyte on the electrochemical synthesis, morphology, and conductivity of polyaniline*, J. Polym. Sci. A Polym. Chem. 1994, **31**(1), 105-111

37. S. Bhadra, N.K. Singha, D. Khastgir, *Electrochemical synthesis of polyaniline and its comparison with chemically synthesized polyaniline*. J. Appl. Polym. Sci. 2007, 1900-1904

38. J. Huang, R.B. Kaner, *A General Chemical Route to Polyaniline Nanofibers*, Journal of the American Chemical Society, 2004, **126**(3), 851-855

39. S.K. Manohar, A.G. Macdiarmid, A.J. Epstein, *Polyaniline: Pernigranile, an isolable intermediate in the conventional chemical synthesis of emeraldine*, Synthetic Metals, 1991, **41**(1), 711-714

40. N.V. Blinova, J. Stejskal, M. Trchová, J. Prokeš, M. Omastová, *Polyaniline and polypyrrole: A comparative study of the preparation*, European Polymer Journal, 2007, **43**(6), 2331-2341

41. M.T. Cortes, E.V. Sierra, *Effect of synthesis parameters in polyaniline: Influence of yield and thermal behavior*. Polymer Bulletin, 2006, **56**(1), 37-45

42. P. Singh, R.A. Singh, *Preparation and characterization of polyaniline nanostructures via a interfacial polymerization method*, Synthetic Metals, 2012, **162**(24), 2193-2200

43. X. Zhang, R. Chan-Yu-King, A. Jose, S.K. Manohar, *Nanofibers of polyaniline synthesized by interfacial polymerization*, Synthetic Metals, 2004, **145**(1), 23-29

44. P. Dallas, D. Stamopoulos, N. Boukos, V. Tzitzios, D. Niarchos, D. Petridis, *Characterization, magnetic and transport properties of polyaniline synthesized through interfacial polymerization*, Polymer, 2007, **48**(11), 3162-3169

45. X. Zhang, W.J. Goux, S.K. Manohar, *Synthesis of Polyaniline Nanofibers by "Nanofiber Seeding"*, J. Am. Chem. Soc., 2004, **126**(14), 4502–4503

46. S. Xing, C. Zhao, S. Jing, Z. Wang, *Morphology and conductivity of polyaniline nanofibers prepared by 'seeding' polymerization*, Polymer, 2006, **47**(7), 2305-2313

47. X. Zhang, S.K. Manohar, *Polyaniline nanofibers: chemical synthesis using surfactants*, Chem Commun. 2004, 2360-2361

48. A.D.W. Carswell, E.A. O'Rear, B.P. Grady, *Adsorbed Surfactants as Templates for the Synthesis of Morphologically Controlled Polyaniline and Polypyrrole Nanostructures on Flat Surfaces: From Spheres to Wires to Flat Films,* Journal of the American Chemical Society, 2003, **125**(48), 14793-14800

49. L. Zhang, M. Wan, *Self-Assembly of Polyaniline—From Nanotubes to Hollow Microspheres*, Adv. Funct. Mater. 2001, **13**(10), 815-820

50. J.H. Cheng, A.F. Fou, M.F. Rubner, *Molecular self-assembly of conducting polymers, Thin Solid Films*, 1994, **244**(1), 985-989

51. L. Zhang, M. Wan, *Chiral polyaniline nanotubes synthesized via a self-assembly process*, Thin Solid Films, 2005, **477**(1), 24-31

52. J. Han, G. Song, R. Guo, *Nanostructure-Based Leaf-like Polyaniline in the Presence of an Amphiphilic Triblock Copolymer*. Adv. Mater. 2007, **19**(19) 2993-2999

53. X. Yu, H. Fan, H. Wang, N. Zhao, X. Zhang, J. Xu, *Self-assembly hierarchical micro/nanostructures of leaf-like polyaniline with 1D nanorods on 2D foliage surface*, Materials Letters, 2011, **65**(17), 2724-2727

54. C.A. Amarnath, J. Kim, K. Kim, J. Choi, D. Sohn, *Nanoflakes to nanorods and nanospheres transition of selenious acid doped polyaniline*, Polymer, 2008, 49(2), 432-437

55. Dhand, C.; Das, M.; Sumana, G.; Srivastava, A. K.; Pandey, M. K.; Kim, C. G.; Datta, M.; Malhotra, B. D. *Nanoscale* **2010**, *2*, 747.

56. M. Yang, X.X. Yao, G. Wang, H. Ding, *A simple method to synthesize sea urchin-like polyaniline hollow spheres*, Colloids and Surfaces A: Physicochemical and Engineering Aspects, 2008, **324**(1), 113-116

57. J. Wang, J. Wang, Z. Wang, F. Zhang, *A Template-Free Method toward Urchin-Like Polyaniline Microspheres*, Macromolecular Rapid Communications, 2009, **30**(8), 604-608

58. R. Nohria, R.K. Khillan, Y. Su, R. Dikshit, Y. Lvov, K. Varahramyan, *Humidity sensor based on ultrathin polyaniline film deposited using layer-by-layer nano-assembly*, Sensors and Actuators B: Chemical, 2006, **114**(1), 218-222

59. Z. Jin, Y. Su, Y. Duan, *Development of a polyaniline-based optical ammonia sensor*, Sensors and Actuators B: Chemical, 2001, **72**(1), 75-79

60. N.E. Agbor, M.C. Petty, A.P. Monkman, *Polyaniline thin films for gas sensing*, Sensors and Actuators B: Chemical, 1995, **28**(3), 173-179

61. S. Takeda, *A new type of CO2 sensor built up with plasma polymerized polyaniline thin film*, Thin Solid Films, 1999, **343**, 313-316

62. Y. Xian, Y. Hu, F. Liu, Y. Xian, H. Wang, L. Jin, *Glucose biosensor based on Au nanoparticles–conductive polyaniline nanocomposite*, Biosensors and Bioelectronics, 2006, **21**(10), 1996-2000

63. M.M. Popović, B.N. Grgur, *Electrochemical synthesis and corrosion behavior of thin polyaniline-benzoate film on mild steel*, Synthetic Metals, 2004, **143**(2), 191-195

64. S.R. Moraes, D. Huerta-Vilca, A.J. Motheo, *Corrosion protection of stainless steel by polyaniline electrosynthesized from phosphate buffer solutions*, Progress in Organic Coatings, 2003, **48**(1), 28-33

65. X.-H. Wang, J. Li, J.-Y. Zhang, Z.-C. Sun, L. Yu, X.-B. Jing, F.-.S. Wang, Z.-X. Sun, Z.-J. Ye, *Polyaniline as marine antifouling and corrosion-prevention agent*, Synthetic Metals, 1999, **102**(1), 1377-1380

66. E. Armelin, Á. Meneguzzi, C.A. Ferreira, C.Alemán, *Polyaniline, polypyrrole and poly(3,4-ethylenedioxythiophene) as additives of organic coatings to prevent corrosion*, Surface and Coatings Technology, 2009, **203**(24), 3763-3769

67. X. Zhang, Z. Liu, Recent advances in microwave initiated synthesis of nanocarbon materials, Nanoscale, 2012, **4**, 707-714

68. M.A. Soto-Oviedo, O.A. Araújo, R. Faez, M.C. Rezende, M.A. De Paoli, *Antistatic coating and electromagnetic shielding properties of a hybrid material based on polyaniline/organoclay nanocomposite and EPDM rubber*, Synthetic Metals, 2006, **156**(18), 1249-1255

69. A.L. Sharma, S. Annapoorni, B.D. Malhotra, *Characterization of electrochemically synthesized poly(2-fluoroaniline) film and its application to glucose biosensor*, Current Applied Physics, 2003, **3**(2), 239-245

70. E. Hür, G. Bereket, Y. Şahin, *Corrosion inhibition of stainless steel by polyaniline, poly(2-chloroaniline), and poly(aniline-co-2-chloroaniline) in HCl*, Progress in Organic Coatings, 2006, **57**(2), 149-158

71. A. Gok, B. Sari, M. Talu, *Polymers, composites, and characterization of conducting polyfuran and poly(2-bromoaniline)*, Journal of Applied Polymer Science, 2005, **98**(5), 2048-2057

72. D. Macinnes Jr., B.L. Funt, *Poly-o-methoxyaniline: A new soluble conducting polymer*, Synthetic Metals, 1988, **25**(3), 235-242

73. J. Yeh, C. Chen, Y. Chen, C. Ma, K. Lee, Y. Wei, S. Li, *Enhancement of corrosion protection effect of poly(o-ethoxyaniline) via the formation of poly(o-ethoxyaniline)–clay nanocomposite materials*, Polymer, 2002, **43**(9), 2729-2736

74. E. Shoji, M.S. Freund, Poly(aniline boronic acid): A new precursor to substiuted poly(aniline)s, Langmuir, 2001, **17**(23), 7183-7185

75. T.L. Porter, P.I. Oden, G. Caple, *Surface structural study of poly-hydroxy-aniline, Surface Science*, 1991, **259**(1), 221-230

76. M. Leclerc, J. Guay, L. H. Dao, *Sythesis and characterization of poly(alkylanilines)*, Macromolecules, 1989, **22**(2), 649-653

77. B.L. Rivas, C.O. Sanchez, *Poly(2-) and (3-aminobenzoic acids) and their copolymers with aniline: Synthesis, characterization, and properties*, Journal of Applied Polymer Science, 2003, **89**(10), 2641-2648

78. C. Barbero, H.J. Salavagione, D.F. Acevedo, D.E. Grumelli, F. Garay, G.A. Planes, G.M. Morales, M.C. Miras, *Novel synthetic methods to produce functionalized conducting polymers I. Polyanilines*, Electrochimica Acta, 2004, **49**(22), 3671-3686

79. C. Han, R. Jeng, *Concurrent reduction and modification of polyaniline emeraldine base with pyrrolidine and other nucleophiles*, Chemical Communications, 1997, 553-554

80. V.V. Paike, R. Balakumar, H. Chen, H. Shih, C. Han, *A serendipitous C-C bond formation reaction between Michael donors and diiminoquinoid ring assisted by quaternary ammonium fluoride*, Organic Letters, 2009, **11**(24), 5586-5589

81. M. Trchva, J. Prokes, I. Sapurina, J. Stejskal, *Brominated Polyaniline*, Chemistry of Materials, 2001, **13**(11), 4083-4086

82. C. Laslau, W. Henderson, Z.D. Zujovic, J. Travas-Sejdic, *Phosphine functionalized polyaniline nanostructures*, Synthetic Metals, 2010, **160**(11), 1173-1178

83. H.J. Salavagione, M.C. Miras, C. Barbero, *Chemical lithography of a conductive polymer using a traceless removable group*, Journal of the American Chemical Society, 2003, **125**(18), 5290-5291

84. Curing agents for Epoxy Resins, Three Bond Technical Report, **32**, 1990